Titre: Title:	Automated Refueling Simulations of a CANDU for the Exploitation of Thorium Fuels
Auteur: Author:	Bradford Holmes
Date:	2013
Type:	Mémoire ou thèse / Dissertation or Thesis
Référence: Citation:	Holmes, B. (2013). Automated Refueling Simulations of a CANDU for the Exploitation of Thorium Fuels [Mémoire de maîtrise, École Polytechnique de Montréal]. PolyPublie. https://publications.polymtl.ca/1307/

UNIVERSITÉ DE MONTRÉAL

AUTOMATED REFUELING SIMULATIONS OF A CANDU FOR THE EXPLOITATION OF THORIUM FUELS

BRADFORD HOLMES

DÉPARTEMENT DE GÉNIE PHYSIQUE

ÉCOLE POLYTECHNIQUE DE MONTRÉAL

MÉMOIRE PRÉSENTÉ EN VUE DE L'OBTENTION

DU DIPLÔME DE MAÎTRISE ÈS SCIENCES APPLIQUÉES

(GÉNIE ÉNERGÉTIQUE)

DÉCEMBRE 2013

UNIVERSITÉ DE MONTRÉAL

ÉCOLE POLYTECHNIQUE DE MONTRÉAL

Ce mémoire intitulé:

AUTOMATED REFUELING SIMULATIONS OF A CANDU FOR THE EXPLOITATION OF THORIUM FUELS

présenté par : HOLMES Bradford

en vue de l'obtention du diplôme de : Maîtrise ès sciences appliquées

a été dûment accepté par le jury d'examen constitué de :

M. MUREITHI Njuki-William, Ph.D, président

M. KOCLAS Jean, Ph.D, membre et directeur de recherche

M. HÉBERT Alain, Doct., membre et codirecteur de recherche

M. TEYSSEDOU Alberto, Ph.D, membre

DEDICATION

Dedicated to my friends and family.

ACKNOWLEDGMENTS

Firstly, I would like to thank Jean Koclas for accepting me as his student and for providing direction and support throughout the project. I would also like to thank Alain Hebert for his help and advice. Also, I thank the rest of the department for the good advice and help in all aspects of completing this degree.

I would like to thank the students in the lab for the collaboration and support throughout the courses and projects for a mutually beneficial experience.

Lastly, I would like to thank my family and friends for the guidance and advice that is always acknowledged and appreciated.

RÉSUMÉ

Les réacteurs nucléaires CANDU ont la caractéristique unique de pouvoir utiliser et exploiter différentes options ou choix de combustibles afin de produire de la puissance électrique utilitaire. Le Thorium, un isotope fertile naturel, est une option qui doit être explorée. Le thorium est plus abondant que l'Uranium, qui est le combustible type actuellement utilisé. De plus, le Thorium est disponible dans de nombreux pays qui désirent développer l'énergie nucléaire.

Ce document est l'aboutissement d'un projet qui explore, teste et analyse la faisabilité de l'utilisation du thorium dans un réacteur CANDU. Dans le cadre de ce projet, nous avons premièrement développé un ensemble de calculs de réseau bidimensionnels et de calculs de mécanismes de réactivité tridimensionnels en utilisant le code DRAGON4. Cette étape est répétée pour plusieurs concentrations de thorium. Les données générées par ces calculs sont par la suite utilisées pour déterminer un enrichissement opérationnel du thorium. Cette recherche est effectuée par une procédure d'élimination et d'optimisation de certains paramètres clés incluant, mais non limité, au burnup moyen et à l'évolution de la réactivité. À cette fin, le projet a permis de déterminer qu'un enrichissement de 1 % du thorium était viable.

Les calculs de coeur complet ont été réalisés par le code DONJON4. Un programme qui simule les opérations de rechargement dans un réacteur CANDU pour ce type de combustible a été développé et a été exécuté pour une période de simulation d'une centaine de jours. Le programme et la sélection en combustible ont satisfait toutes les conditions fixées sur la totalité de la période de simulation. Le programme nécessitera davantage d'optimisation avant qu'il puisse être largement utilisé.

La sélection de combustible a également été examinée dans le cas où une insertion de réactivité est simulée. Le retrait de la barre de compensation numéron 11 a été analysé et comparé à un cas classique CANDU antérieur afin de s'assurer de l'absence de déviations ou d'évolutions indésirables. Dans ce cas, les résultats de la simulation ont été trouvés acceptables, sans déviations sensibles par rapport au cas classique CANDU.

ABSTRACT

CANDU nuclear reactors are in a unique circumstance where they are able to utilize and exploit a number of different fuel options to provide power as a utility. Thorium, a fertile isotope found naturally, is one option that should be explored. Thorium is more abundant than uranium, which is the typical fuel in the reactor and the availability of thorium makes nuclear energy desirable to more countries.

This document contains the culmination of a project that explores, tests, and analyzes the feasibility of using thorium in a CANDU reactor. The project first develops a set of two-dimensional lattice and three dimensional control rod simulations using the DRAGON Version 4 nuclear physics codes. This step is repeated for many concentrations of thorium. The data generated in these steps is then used to determine a functional enrichment of thorium. This is done via a procedural elimination and optimization of certain key parameters including but not limited to average exit burnup and reactivity evolution. For the purposes of this project, an enrichment of 1 % thorium was found viable.

Full core calculations were done using the DONJON 4 code. CANFUEL, a program which simulates the refueling operations of a CANDU reactor for this fuel type was developed and ran for a simulation period of one hundred days. The program and the fuel selection met all selected requirements for the entirety of the simulation period. CANFUEL requires optimization for fuel selection before it can be used extensively.

The fuel selection was further scrutinized when a reactivity insertion event was simulated. The adjuster rod 11 withdrawal from the core was analyzed and compared to classical CANDU results in order to ensure no significant deviations or unwanted evolutions were encountered. For this case, the simulation results were deemed acceptable with no significant deviations from the classical CANDU case.

TABLE OF CONTENTS

LIST OF TABLES

LIST OF FIGURES

LIST OF ANNEXES

LIST OF ABREVIATIONS

CANDU	Canadian Deuterium Uranium
tU	tonnes uranium
GWe	giga-watt electric
MWth	mega-Watt thermal
MWd/MTHE	mega-Watt days per metric tonne heavy element
TAV	Time-average
INST	Instantaneous
LZC	Liquid Zone Controller
MCA	Mechanical Control Rod
SOR	Shut Off Rod
MC	Monte-Carlo
FPD	Full Power Day
CPPF	Channel Power Peaking Factor
HFP	Hot Full Power
k-eff	k-effective
LAB	Laboratory frame of reference

Chapter 1. **INTRODUCTION**

1.1 Thorium as a Fuel

The nuclear power industry has been using uranium as the primary source of fuel since reactor technology first created a useful cycle for power production. Uranium-235 (^{235}U), a fissile isotope is fissioned within the core and the energy released by fission is eventually transformed into more useful electricity. However, it has been determined through research and future projections that uranium will be harder to acquire at a low price for fuel in new nuclear reactors [1,2]. To compensate for the unavoidable decline in available natural uranium, thorium has been proposed as an alternative breeder fuel source [3,4]. Globally, there are approximately 435 nuclear reactors in operation with a combined electrical capacity exceeding 370 GWe. Combined, these reactors require about 77 000 tonnes of uranium oxide concentrate, and about 65 500 tonnes of uranium (tU) each year. It is forecasted that each electric gigawatt (GWe) of additional capacity will require an additional 195 tU mined per year, based solely on routine mining operations and disregarding initial fuel loading. Global supplies of uranium are finite and are approaching peak availability rapidly.

Thorium-232 (^{232}Th) is a naturally-occurring nuclide that is the most abundant of all thorium isotopes. It is of particular interest as a nuclear fuel source due to ^{232}Th being a fertile nuclide, and its relative abundance when compared to naturally-occurring uranium ore. Comparatively, Canada's estimated stores of uranium total approximately 500 000 metric tonnes [1]. This supply is predicted to place Canada in the forefront of future uranium exploration and production. Thorium's breeding capacity results from neutron absorption into ^{232}Th. Thorium decays into protactinium-233 (^{233}Pa) and then into uranium-233 (^{233}U), a fissile long-lived isotope. This process is shown in the radiological decay chain below:

$$\mathrm{Th}^{232} + n^{1} \rightarrow \mathrm{Th}^{233} \xrightarrow{22\ \mathrm{min}} \mathrm{Pa}^{233} \xrightarrow{27\ \mathrm{days}} \mathrm{U}^{233} \tag{1.1}$$

The added neutron economy is considered to be a major asset to thorium as a breeder in our simulations.

As of now, studies that involve thorium are being conducted using the CANFLEX fuel type. This fuel relies on uranium enrichment and an increase in the number of fuel pins and a burnable poison in the center pin. Greater fuel irradiations can be achieved; however, the need for enrichment limits the availability to prospective users of the fuel.

1.2 Objective

The goal of this study was to develop, test, and validate computational schemes using the CLE-2000 scripting language for the purpose of introduction of natural thorium into typical 37-element fuel bundles in a CANDU-6 reactor. Further, the computational schemes are used to determine the reactor kinetics responses of a reactivity insertion, and compare them to the response of the CANDU-6 reactor. These efforts are directed into making the CANDU-6 reactor more appealing to parties which are interested in the use of thorium as a fuel due to its inherent benefits.

To the aid of this report, reactor physics codes DRAGON and DONJON Version 4 will provide the necessary solutions to the neutron transport equations for cells and assemblies, and the solutions to the neutron diffusion equations for finite reactor analysis respectively [5,6]. DRAGON and DONJON were created partly to develop a nuclear analysis capability to support technical requirements of nuclear plant operations at the Gentilly-2 station, owned by Hydro-Québec.

The method by which this was accomplished started with the development of a 2-dimensional cell that calculates isotopic contents and subsequent macroscopic mixture cross-sections based on a multigroup neutron flux normalized to a specific heavy element fission power, and fuel irradiation. DRAGON solves the neutron transport calculation using the collision probability method with reflective boundary conditions. These calculations are verified by existing results available in the literature and Monte Carlo calculations performed with code SERPENT [7].

A 3-dimension cell was required for the calculation of incremental macroscopic cross-sections of the insertion and removal of reactivity devices. These reactivity devices include adjusters and Liquid Zone Controllers (LZC) as well as necessary guide tubes.

Full core calculations are composed of two sets of calculations: Time-averaged (TAV) calculations and Instantaneous (INST) calculations. TAV calculations are required to develop a

reference “average” or equilibrium which can be compared to for instantaneous calculations. This involves a core that has two separate burnup zones which allow some optimization of the average exit burnup of the channels. The INST calculations provide a more realistic view of the reactor. The reactor is continually refueled from a reference state to an equilibrium state, close to that of the TAV model, using an automated refueling program CANFUEL. From this state, reactor kinetics calculations were performed and compared to nominal CANDU-6 responses.

1.3 Outline

Chapter 2 covers the theories and concepts needed to understand the content of the remainder of the report. This should be used a reference and it should be noted that no new material is in this section. Chapter 3 introduces and explains the CANDU-6 reactor and how various models are used to create an accurate representation of the neutron physics of core and cell geometries. In Chapter 4, the fuel selection criteria, studies and final selection is documented. In Chapter 5, the automated refueling program CANFUEL is described in terms of methodologies, restrictions, and results. The reactivity insertion event is studied and compared to nominal CANDU-6 reactor kinetics and implications in Chapter 6. The conclusion ties the report together and makes suggestions on where the project should go next.

Chapter 2. **REACTOR PHYSICS CONCEPTS**

This chapter is required for a full understanding of the research conducted and presented in this report. It focuses on the methods and equations required to solve the neutron transport and neutron diffusion equations. This can be generalized to reactor physics. Reactor physics in the context of nuclear power generation describes the interaction between neutrons and matter. Neutrons collide with the nucleus of particles present in the reactor to produce a variety of outcomes. These outcomes are based on the energy of the colliding neutron and the characteristics of the nuclide in question. In order to extract power from fission energy, many interactions must take place, specifically fission. The neutron number density can be obtained as the solution to the transport equation. In order to successfully solve the neutron transport equation, several factors are required and will be developed in this section. Source density, transport correction, neutron leakage, multigroup discretization, and material cross-sections are necessary to solve for a static case. Perturbations to the reactor require additional information that can be determined using space-time kinetics. For a more in depth and complete description of these theories, please look to books by Alain Hebert and Daniel Rozon [8,9].

It is not practical to account for all realistic scenarios of the particles or neutrons. Several assumptions can be made without affecting the reliability of the solutions:

- Relativistic effects can be ignored
- Neutron-neutron interactions can be ignored
- Neutrons are neutral particles and neutron mean free paths are straight lines
- Reactor materials are isotropic in space
- Nuclides are in thermal equilibrium within mixture definitions

2.1 Particle Flux

The particle flux within a reactor is the description of the particle density in the context of the transport equation. The description of a single particle is defined by a set of seven quantities:

- Three position coordinates $\mathbf{r} = x\,\mathbf{i} + y\,\mathbf{j} + z\,\mathbf{k}$

- Three velocity coordinates. These include the velocity module $V_n \equiv |\mathbf{V_n}|$ with $\mathbf{V_n} = d\mathbf{r}/dt$ and the two direction components $\mathbf{\Omega} \equiv \mathbf{V_n}/V_n$
- The time *t*.

The particle density $n(\mathbf{r},V_n,\mathbf{\Omega},\mathrm{t})$ is represented as a distribution and can be described further such that $n(\mathbf{r},V_n,\mathbf{\Omega},\mathrm{t})d^3rdV_nd^2\Omega$ is the number of partiles at time t, in the volume element d^3r surrounding point **r**, in the velocity element dV_n surrounding V_n, and in the solid angle element $d^2\Omega$ surrounding $\mathbf{\Omega}$. The particle density is a distribution of all factors except t, in which it is a function of.

The particle density can be made more useful by using it to define the angular flux and the integrated flux respectively, as shown below:

$$\phi(\mathbf{r},V_n,\mathbf{\Omega},\mathrm{t}) \equiv V_n n(\mathbf{r},V_n,\mathbf{\Omega},\mathrm{t}) \tag{2.1}$$

$$\phi(\mathbf{r},V_n,\mathrm{t}) = \int_{4\pi} d^2\Omega\phi(\mathbf{r},V_n,\mathbf{\Omega},\mathrm{t}) \tag{2.2}$$

It may be more convenient to describe the flux in terms of particle energy E or lethargy u by replacing V_n. Taking note that the particle speed is a distribution, the change of variables resolves as;

$$E = \frac{1}{2}mV_n^2 \text{ and } u = \ln\frac{E_0}{E} \tag{2.3}$$

where m is the mass of the particle and E_0 is the maximum energy of the particle.

The angular current, which is described as a distribution of the number of particles per element of time dn/dt of velocity V_n, and direction $\mathbf{\Omega}$, crossing a surface d^2S. With this, we also have the integrated current crossing the surface. A positive current is the particle flux heading in positive direction defined by the positive normal to the surface and the negative current is the particle flux heading in the negative direction defined by the negative normal to the surface. Both angular and integrated current are defined below respectively;

$$\boldsymbol{J}(\mathbf{r},V_n,\mathbf{\Omega},\mathrm{t}) \equiv \mathbf{\Omega}\phi(\mathbf{r},V_n,\mathbf{\Omega},\mathrm{t}) \tag{2.4}$$

$$\boldsymbol{J}(\mathbf{r},V_{\boldsymbol{n}},\mathrm{t}) = \int_{4\pi} d^2\boldsymbol{\Omega}\boldsymbol{J}(\mathbf{r},V_{\boldsymbol{n}},\boldsymbol{\Omega},\mathrm{t}) = \int_{4\pi} d^2\Omega\boldsymbol{\Omega}\phi(\mathbf{r},V_{\boldsymbol{n}},\boldsymbol{\Omega},\mathrm{t}) \tag{2.5}$$

2.2 Nuclear Cross Sections

A nuclear cross section is simply the probability of a specified reaction to occur during a neutron nucleus collision. First, we take a parallel beam of mono-energetic neutrons, I per unit surface and unit time and target a homogenous material with density N particles per cubic centimeter. A reaction x will occur at a rate dR_x which can be calculated using the microscopic cross-section for the specified reaction shown below:

$$dR_x = \sigma_x NIds \tag{2.6}$$

This cross section is expressed in barns, which is 10^{-24} cm^2. The macroscopic cross-section will take into account the entirety of the target and will then have units of cm^{-1}.

$$\Sigma_{\mathrm{x}} = N\sigma_x \tag{2.7}$$

2.3 Transport Equations

The transport equation is a balance of particles within an arbitrary control volume for a time that does not result in significant changes to the cross-sections of the materials. It is described in four terms, namely; the rate change of particles, the number of particles streaming out of the control volume, the number of collisions, and the number of new particles created. This equation is shown below:

$$\frac{\mathbf{1}}{V_{\boldsymbol{n}}}\frac{\partial}{\partial \mathrm{t}}\phi(\mathbf{r},V_{\boldsymbol{n}},\boldsymbol{\Omega},t) + \nabla\cdot\boldsymbol{\Omega}\phi(\mathbf{r},V_{\boldsymbol{n}},\boldsymbol{\Omega},t) + \Sigma(\mathbf{r},V_{\boldsymbol{n}})\phi(\mathbf{r},V_{\boldsymbol{n}},\boldsymbol{\Omega},t) = \mathrm{Q}(\mathbf{r},V_{\boldsymbol{n}},\boldsymbol{\Omega},t) \tag{2.8}$$

During steady state conditions, the equation may be written as;

$$\boldsymbol{\Omega}\cdot\nabla\phi(\mathbf{r},V_{\boldsymbol{n}},\boldsymbol{\Omega}) + \Sigma(\mathbf{r},V_{\boldsymbol{n}})\phi(\mathbf{r},V_{\boldsymbol{n}},\boldsymbol{\Omega}) = \mathrm{Q}(\mathbf{r},V_{\boldsymbol{n}},\boldsymbol{\Omega}) \tag{2.9}$$

2.4 Source Density and Transport Correction

The source density accounts for secondary neutrons created by either fission or scattering reactions. Scattering reactions will include collisions that produce a neutron with a different energy than it began with, usually with a lower energy or a higher lethargy and (n,xn) reactions. The steady-state scattering source is described as:

$$\mathrm{Q}(\mathbf{r},E,\boldsymbol{\Omega})^{\mathrm{scat}} = \int_{4\pi} d^2\boldsymbol{\Omega}' \int_0^{\infty} dE' \Sigma_{\mathrm{s}}(\mathbf{r}, E \leftarrow E', \boldsymbol{\Omega}\cdot\boldsymbol{\Omega}')\, \phi(\mathbf{r},E',\boldsymbol{\Omega}') \tag{2.10}$$

where

$\Sigma_{\mathrm{s}}(\mathbf{r}, E \leftarrow E', \boldsymbol{\Omega}\cdot\boldsymbol{\Omega}')$ = the macroscopic scattering cross-section that accounts for diffusion and (n,xn) reactions.

The fission source term can be assumed to be isotropic in the LAB and is independent of incident neutron direction. The fission neutrons are emitted as a distribution of energy defined as the fission spectrum $\chi_i(E)$. The spectrum for all possible neutron emission energies is normalized to 1. Thus, the isotropic fission source can be written as;

$$\mathrm{Q}(\mathbf{r},E)^{\mathrm{fiss}} = \sum_{\mathrm{j}=1}^{\mathrm{J}^{\mathrm{fiss}}} \chi_j(E) \int_0^{\infty} dE' \nu\Sigma_{\mathrm{f,j}}(\mathbf{r},E')\, \phi(\mathbf{r},E') \tag{2.11}$$

where

$\mathrm{J}^{\mathrm{fiss}}$ = total number of fissile isotopes.

$\nu\Sigma_{\mathrm{f,j}}(\mathbf{r},E')$ = the number of emitted neutrons per fission times the macroscopic fission cross-section for the j^{th} isotope.

While the fission source can be considered isotropic, scattering reactions are not. This can be accounted for with the use of the transport correction on the cross sections in the transport equation. To have an equation that depicts a more realistic outcome, a forward peaking component in the Legendre expansion of the differential scattering cross-section is added. This is shown as:

$$\Sigma_{\mathrm{s}}(\mathbf{r}, E \leftarrow E', \mathbf{\Omega}) = \sum_{l=0}^{\mathrm{L}} \frac{2l+1}{2} \bar{\Sigma}_{\mathrm{s},l}(\mathbf{r}, E \leftarrow E') P_l(\mu) + \Delta\Sigma_{\mathrm{tr}}(\mathbf{r}, E \leftarrow E')\delta(\mu - 1) \tag{2.12}$$

Where the two cross-sections on the right hand side of the equation are the modified Legendre coefficient and addition coefficient multiplied by the dirac delta term, respectively. The coefficients are calculated to preserve the Legendre moments and will not be covered here. However, the transport-corrected steady-state source density is presented below:

$$\begin{aligned} \bar{\mathrm{Q}}(\mathbf{r}, E, \mu) = \frac{1}{4\pi} \int_0^{\infty} dE' \bar{\Sigma}_{\mathrm{s},0}(\mathbf{r}, E \leftarrow E') \phi(\mathbf{r}, E') \\ + \frac{1}{4\pi K_{eff}} \sum_{\mathrm{j}=1}^{\mathrm{J^{fiss}}} \chi_j(E) \int_0^{\infty} dE' \nu\Sigma_{\mathrm{f,j}}(\mathbf{r}, E') \phi(\mathbf{r}, E') \end{aligned} \tag{2.13}$$

where the P_0 transport-corrected component of the differential scattering cross-section is written below:

$$\Sigma_{\mathrm{s},0}(\mathbf{r}, E \leftarrow E') = \bar{\Sigma}_{\mathrm{s},0}(\mathbf{r}, E \leftarrow E') + \Delta\Sigma_{\mathrm{tr}}(\mathbf{r}, E)\delta(E' - E) \tag{2.14}$$

2.5 Boundary Calculations and Leakage

To limit the resources required to obtain the desired results, a cell assembly is implemented to contain one "unit cell" of the CANDU reactor. This cell is one lattice pitch in length and width and contains the fuel assembly, tubing, and moderator. To simulate an infinite reactor, certain boundary conditions are applied to the unit cell. The albedo boundary condition relates the incoming flux with a known outgoing flux as such:

$$\phi(\mathbf{r_s}, V_{\boldsymbol{n}}, \mathbf{\Omega}, t) = \beta\phi(\mathbf{r_s}, V_{\boldsymbol{n}}, \mathbf{\Omega}', t) \text{ with } \mathbf{\Omega} \cdot \mathbf{N}(\mathbf{r_s}) < 0 \tag{2.15}$$

where β is set to one to indicate a reflective boundary condition which helps to simulate an infinite lattice. The reflective boundary acts as a mirror reflection to neutrons incident on the boundary.

To model a more realistic reactor, one which has a k-eff equal to one, buckling is imposed. For this case, the fundamental mode approximation must be made. This means that the

flux is represented as the macroscopic distribution in space $\psi(\mathbf{r})$ and a periodic fundamental flux $\varphi(\mathbf{r}, E, \mathbf{\Omega})$ which can be written as:

$$\phi(\mathbf{r}, E, \mathbf{\Omega}) = \psi(\mathbf{r})\, \varphi(\mathbf{r}, E, \mathbf{\Omega}) \tag{2.16}$$

With this, the macroscopic distribution can be considered a property of the complete reactor and a solution to the following Laplace equation:

$$\nabla^2 \psi(\mathbf{r}) + B^2 \psi(\mathbf{r}) = 0 \tag{2.17}$$

where the buckling B^2 is a real number and is used to adjust the curvature of the distribution in order to achieve a critical reactor.

2.6 Multigroup Discretization

It is necessary, due to resource constraints, to divide the energy domain into subsections known as groups. Within each group, it is assumed that the neutrons found within the boundaries of the group have one speed, instead of a distribution of speeds. That speed corresponds to the average energy of neutrons within that group. There are 8 delayed neutron groups in accordance to the Jef 3.1.1 libraries [10]. A further condensation is required to complete the solution to the diffusion equation during full core calculations. Since we are operating with a CANDU reactor and the moderating ratio is quite large, it is typically accepted that 2 groups are all that is necessary [11]. These two groups are divided into fast and thermal neutrons, the energy of discrimination being 4 eV.

2.7 Collision Probability Method

The collision probability method was used in this report to determine the collision probabilities of the unit cell with a number of regions V_i over an infinite reflective lattice. The collision probability $P_{ij,g}$ is defined as the probability of a neutron born uniformly and isotropically in a region V_i to undergo its first collision in a region V_j of the unit cell. The collision probability is calculated based on a number of tracks which relies on the azimuthal angles and tracking density specified. This information is then used in conjunction with the macroscopic cross-sections for each region at each energy group to compute the collision probabilities. Thus, the integrated flux can then be calculated.

2.8 Burnup

Fuel burnup is the measure of energy released by fuel per unit mass of uranium during the time spent in the reactor and can be referred to as another measure of fuel irradiation time. However, the burnup of nuclear fuel is proportionally related to the time spent in the reactor. The relation between the burnup and time spent in the reactor is not exactly equivalent due to localized flux variations and therefore it is inappropriate to compare different fuel types with different enrichment levels and to effectively equate burnup to time spent in the reactor.

Fuel burnup is defined as the amount of fission energy produced by the fuel from the time it has entered into the reactor. It is measured as the energy produced per unit mass of original heavy element and has the common unit of megawatt-days per metric tonne heavy element (MWd/MTHE). In the case of thermal reactors, the heavy elements of interest are the fissile isotopes, uranium-235 and plutonium-239. Burnup is therefore a product of the reactor's thermal power (P, MWth), the time the fuel has been irradiated in the reactor (t, days), the capacity factor of the reactor, and the original unit mass of heavy element (m, MWd/MTHE) related as follows;

$$Fuel\ Burnup = \frac{P \times CF \times t}{m} \tag{2.18}$$

This relation is only valid for the measure of burnup for the original heavy element fed into the reactor – it does not account for the production of any fissile isotopes due to fuel irradiation. The resonance absorption of uranium-238 atoms results in a noticeable fission yield of plutonium-239. The production of plutonium-239 adds to the quantity of fissile material and will further enhance the infinite-cell multiplicative factor.

2.9 Monte Carlo Method

The Monte-Carlo method is another approach which can be used to solve the neutron transport equation. The method obtains answers using the simulation of individual particles and recording the average behaviour of the particles in question. If the number of tracked histories is high

enough, it can often be similar to conducting an experiment. The physics of the code includes the following; weight, particle tracks, and neutron interactions. The weight is an individual particle or source contribution to the average. Realistically, this weight would be a unit weight per particle, however it is possible to assign a particle source unit weight for computational efficiency. The collective weight of particles will make up the pulse height.

Particle tracks start when a particle leaves the source and is subsequently tracked. Once the particle interacts with a material, a new track is started. If the interaction would induce additional particles in the material, subsequent tracks are then also initiated. Track lengths tallies are then used to determine important information from the system such as fluence, flux, and energy deposition. If the cell is a fixed homogenous region, the probability of the first collision can be determined by the following equation:

$$p(l)dl = e^{-\Sigma_l \Sigma_t dl} \tag{2.19}$$

where Σ_t is the macroscopic total cross section of the medium and is interpreted as the probability per unit length of a collision and l is the length.

Neutron interactions occur when a neutron collides with a nucleus. The nuclide is identified and the reaction is treated to determine the resulting outcome of the collision. The results are based on the specified treatment and cross-sections of the material along with the weight, random number, nuclide size, and incident neutron energy.

Chapter 3. **MODELING THE CANDU**

To model the CANDU reactor and the fuel within, the DRAGON and DONJON Version 4 set of codes were used [5,6]. In the case of the fuel cell, a validation simulation was performed using SERPENT.

DRAGON is an open source software package that contains a collection of modules that can simulate the neutron behavior of a unit cell or a fuel assembly in a nuclear reactor [5]. It includes all of the functions that characterize a lattice cell code, namely: the interpolation of microscopic cross sections supplied by means of standard libraries; resonance self-shielding calculations in multidimensional geometries; multigroup and multidimensional neutron flux calculations.

DONJON is its sister program, designed to for the full reactor core modeling in 3D Cartesian and other geometries [6]. The modeling of the fuel lattice is done through defining the number of channels and bundles for each channel and each channel is recognized by specified names. Using either instantaneous or time-average methods, the interpolation of fuel properties with respect to fuel burnup can be achieved.

Reactivity control mechanisms are modeled using their material properties and position. SERPENT is a Monte-Carlo based program that models the infinite lattice of the fuel cell and is used to validate DRAGON calculations [7].

3.1 2D Lattice Calculations

The 2D lattice cell calculation is used to generate burnup dependent characteristics of the fuel. The cell consists of the fuel bundle, coolant and fuel channel tubing, and the surrounding moderator. The geometry is defined by the 37-element fuel bundle and CANDU reactor design [12]. Using the 281 group DRAGLIB library, JEFF 3.1.1, the material cross-sections are defined by their isotopic makeup and adjusted for temperature [10]. A sample of the geometry is included in the Figure 3.1.

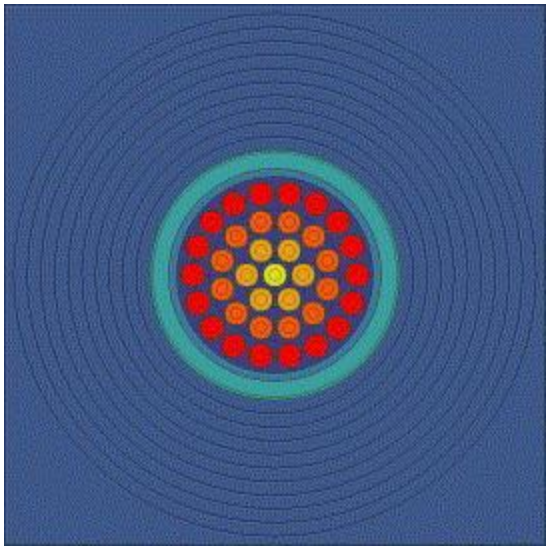

Figure 3.1 37-Element CANDU Fuel Representation.

To obtain an accurate representation of the reactor from this geometry, reflective boundary conditions are applied to the cell with a B1 buckling set to a critical reactor, k-eff= 1. Self-shielding effects are applied to the cell during calculations using the USS: module. This will apply corrections to the microscopic cross-sections based on the self-shielding effect of resonant isotopes. The cell is then burned at a constant power 32 MWd/MTHE until an appropriate burnup is reached.

The 2D cell is the basis for the majority of the calculations required in this study. It is important that all the required data is stored and easily accessible for future use and consultation. This is done through the CPO: module. This is a database that stores homogenized cell data based on burnup or irradiation. The alternative method is to use the COMPO: module which stores all of the nuclear data produced in the lattice code. This is most effective when multiple parameters are being changed and all data needs to be stored. It is useful in this study where multiple initial concentrations of thorium are tried to determine an effective implementation in the CANDU reactor. Further implications could include a change in lattice pitch and fuel geometry such as the CANFLEX fuel design but are not within the scope of this study. Once the data is exported, it is now useful in modeling reactivity devices and a full core.

3.2 3D Modeling of a Reactivity Device

In order to properly model a full core, the inclusion of reactivity devices must be properly accounted for. This is done using DRAGON Version 4, taking advantage of the 3D Cartesian options in the GEO: module. Specifically, Mechanical Control Absorbers (MCAs), Adjuster Rods, and Liquid Zone Controllers (LZC) must be modeled. There are 4 MCAs which are provided as part of the reactor regulating system. They are physically identical to the Shut Off Rods (SORs) and are normally located outside the core. The Adjuster Rods are normally fully inserted in the core and are meant to be a shim for flux flattening. They are housed within a stainless steel tube. The LZCs are a mixture of water and helium and are located within the 14 zones of the core. They are meant to be a fine reactivity control for their respective zones and ensure an even burn of the fuel in that region with respect to the reactor.

Calculations are preformed using the 3D Cartesian geometry that spans two lattice pitches in width and one in height, as well as one fuel bundle length in depth (57.150 cm x 28.575 cm x 49.520 cm). This model is shown in Figure 3.2.

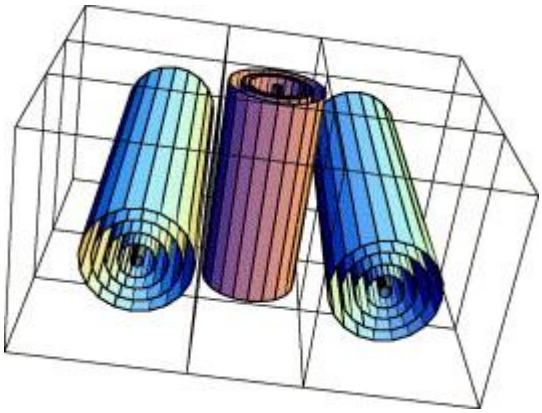

Figure 3.2. Reactivity Device Modeling in DRAGON.

The fuel in this figure is taken from data obtained within the 2D lattice calculations and is homogenized for computational efficiency. The device is modelled in the center of the two fuel assemblies at various states to obtain differential cross-section data [13,14]. The states include a natural supercell with no device or housing and then progress to include only the housing and finally the housing and a fully inserted device. Two group energy condensations are used in accordance with the literature for a CANDU reactor [11].

After modeling, it is important to determine and store the incremental cross-section information for each device. This involves taking the 3-D geometry with the two fuel bundles and determining the incremental cross-section by simulating with the reactivity device fully inserted and then again with the device absent. The difference between the two results provides the incremental cross-sections which are used in full core calculations. Determining the device worth for LZC is done by creating a full core snapshot of a critical reactor with all controllers at 50% full. Devices are then inserted and then fully removed to determine the effect on reactivity in the core. The global reactivity worth of the devices can be determined from the perturbed reactivities as:

$$\rho = \left(\frac{1}{k_{eff,ref}} - \frac{1}{k_{eff,per}}\right) \tag{3.1}$$

The total reactivity worth of the LZC in a CANDU core with typical fuel is often stated as roughly 7 mk. With the introduction of thorium into the lattice, the reactivity device worth is diminished [15]. For the fuel chosen, the total device worth of the LZC is 6 mk. This is consistent with the results above.

3.3 Full Core Calculations

The CANDU core contains 380 horizontal channels which contain 12 fuel bundles each. The fuel bundles are comprised of a uranium oxide pellets in each fuel pin. The core is divided into 14 zones for fine reactivity control and flux mapping. Within the core are 14 LZCs, 21 adjuster rods, and 4 MCAs which have been modeled and homogenized using the DONJON code. The time-averaged (TA) model and the instantaneous models are used to reference and describe the full core characteristics [16].

The time-averaged model of the CANDU is used to compute the burnup integration limits for each fuel bundle, the axial power-shape over the fuel lattice, the channel refuelling rates and the reactor core-average exit burnup [11]. The calculations are performed using equilibrium core conditions with the LZC set to 50% full. A bidirectional refueling scheme is used on a two-zone average exit burnup layout.

For the purposes of this project, TA calculations are used as reference results set to be nominal operations. Channel and zone powers will be used to compare instantaneous results to in

order to determine LZC levels and required zone reactivity for refuelling. The average exit burnups for the two burnup zones, will be used for determining channels that are required for refuelling in the refueling program. Core maps describing the regional zones and burnup zones are provided in Appendix 1.

There are two types of instantaneous calculations. The first is a random distribution based on burnup of the TA core. This is the starting point for the refueling simulation as well as decent projection of nominal power distribution within the core. This is done by finding the average exit burnup of the zone and then applying a large number of averaged random weightings to each channel to define an instantaneous channel burnup. After this is done for each channel in its respective zone, the instantaneous core calculation can be performed and the axial power shape should be very close to that of the TA calculation. Of course, each calculation is normalized to the total reactor power. Core decay and channel refuelling as well as accident type scenarios can then occur from this state.

3.4 Monte Carlo Validation

A benchmark simulation must be done in Monte Carlo (MC) in order to validate the results given in DRAGON. For this project, SERPENT was used to obtain these results. The geometry and boundary conditions were made identical to DRAGON calculations for the benchmark simulations. According to best practices, there are three main concerns that must be addressed when performing MC; sufficient initial cycles must be discarded prior to beginning the tallies in order to avoid contamination from initial guesses, a sufficient number of neutrons must be followed in each cycle so that the bias in reaction rate and k-eff are negligible, and the bias in the statistics must be recognized and dealt with [17]. From this, it is recommended that 10 000 or more neutrons per cycle be used in two-dimensional lattice calculations. The validation simulations used 500 cycles and followed 20 000 source neutrons while the first 10 cycles were discarded. The convergence on k-eff with the number of cycles is shown in the figure below.

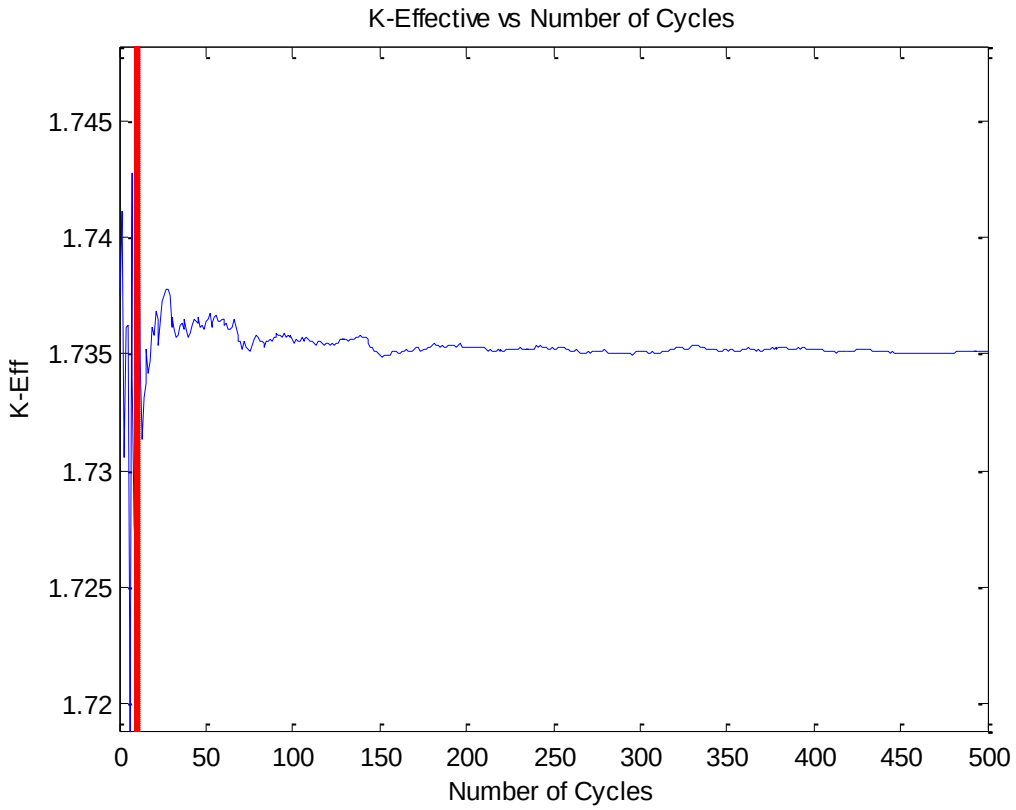

Figure 3.3 Monte Carlo Convergence on k-eff for Uranium and Thorium Enriched Fuel.

Enrichment of both uranium and thorium was considered to test the accuracy and benchmark against DRAGON results and is shown in Figure 3.3. The k-eff with a constant neutron weight was obtained from the MC calculations as 1.73509 ± 0.00042. Comparison to the results obtained using DRAGON, for which the k-eff was 1.72972. This yields an error of 0.3% which is determined to be acceptable. Results from DRAGON were generated using the sub-group approach with the 281-group JEFF 3.1.1 DRAGLIB.

Table 3.1. K-eff Results from SERPENT and DRAGON Simulations.

SERPENT k-eff	**DRAGON k-eff**	**Error %**
1.73509 ± 0.00042	1.72972	0.2

Chapter 4. **FUEL SELECTION**

A new fuel selection was made to include fertile thorium-232. Limited data was produced and analyzed due to time constraints. The majority of the project time was spent developing the CANFUEL program which is described in Chapter 5. However, certain objectives were set out to be met and will be explained in the following sections. A selection was made that best met the majority of decision criteria while still maintaining an operational reactor.

4.1 Decision Criteria

A selection for the fuel was made based on the following decision criteria:

- Obtain the highest level of thorium concentration in the fuel
- Use the 37-element CANDU fuel bundle geometry
- Fuel mixture is to be homogeneous in all fuel pins
- Average exit burnup must be as high as possible
- Refueling rate must be similar to that of the CANDU reactor due to limits on the number of refuelings per day determined by the refueling machine
- Fuel must meet safety standards discussed in Section 5

A closer look at some of the effects of each decision point will help to determine the final selection. Thorium, as discussed in the introduction, is a desirable fuel source that can and should be utilized in reactors in the future. The selection will be the fuel source that meets all of the other requirements and has the highest possible thorium concentration. Since we are limited to the CANLUBE fuel bundle with a homogeneous fuel mixture within each pin, the selection variables are as follows; thorium enrichment and the number of bundles replaced during a refueling operation.

Reactivity insertion due to refueling is the main course of reactivity control in the CANDU reactor. It is very important that there is both a positive reactivity insertion due to refueling and that this insertion is enough to compensate for decay reactivity and required zonal reactivity. The enrichment of CANLUBE fuel with thorium causes the reactivity of insertion due to refueling to be smaller, compared to natural uranium. This difference becomes more

significant with higher enrichments and is not compensated for with the production of uranium-233 until much higher burnups. This relation is shown in Figure 4.1. Any fuel containing 10% or more thorium enrichment will not add reactivity to the core.

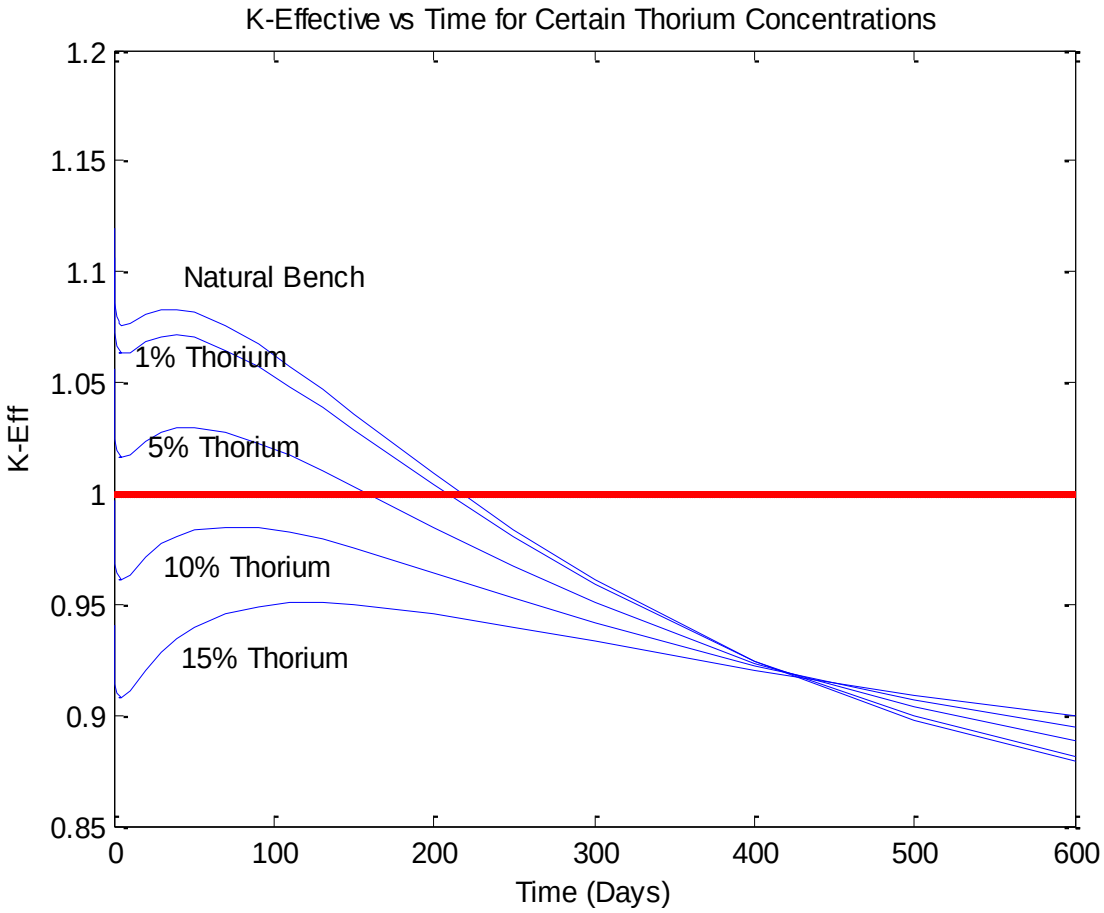

Figure 4.1 K-eff of Selected Fuel Types with Respect to Burnup.

The trend of reduces returns with respect to an increase in thorium concentration is also apparent in the average exit burnup of refueled bundles. A minimum acceptable burnup of 5200 MWD/MTHE was set for the fuel which disregarded any enrichment over 2.5%. All values in Figure 4.2 are for an 8 bundle shift.

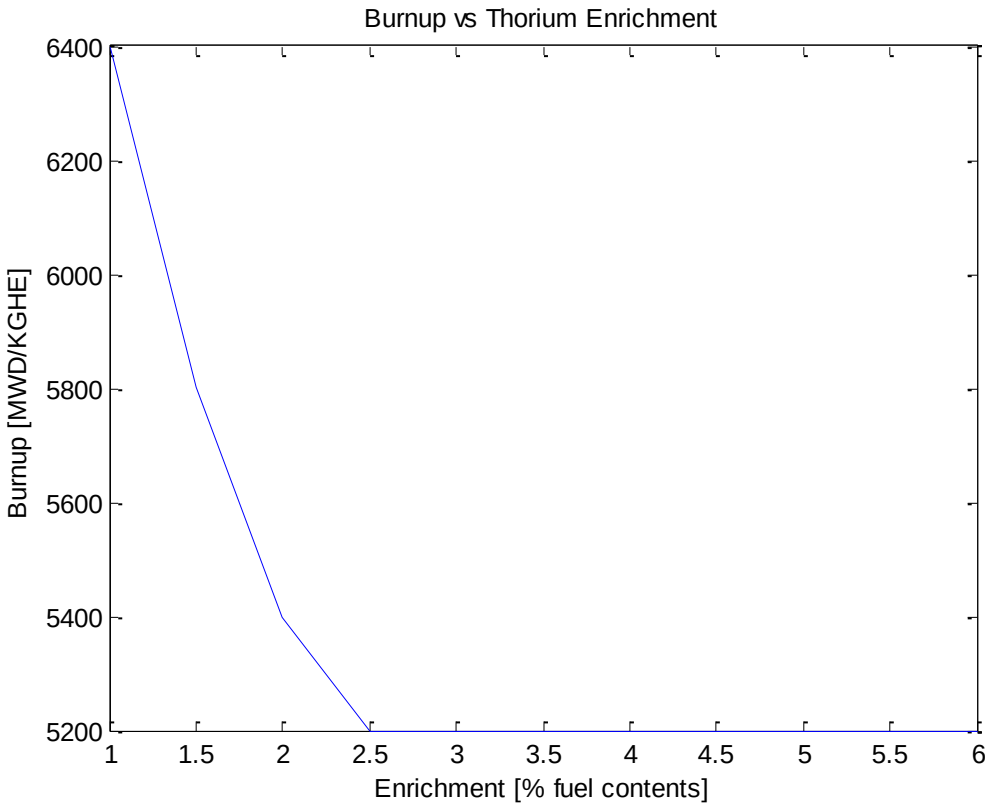

Figure 4.2. Average Exit Burnup Compared to Throium Enrichment.

In order to reduce fueling costs, exit burnup should be as high as possible. An increased burnup of the fuel indicated a longer residency time which means less fuel is required to refuel the reactor. Lowering the number of bundle shifts will increase the exit burnup of the fuel but increase the refueling rate and put additional strain on the refueling machine. Therefore it is desirable to achieve burnup and refueling rates that are similar to the CANDU but have an increase in thorium enrichment. The refueling rate for a CANDU today is roughly 2.2 refueling procedures of 8 bundles per day.

4.2 Fuel Selection

Based on these criteria, an enrichment of 1% with an 8-bundle shift was chosen. This provided an average refueling rate of 2.27 refueling procedures per day and an average exit burnup of 5992.57 MWd/MTHE. The average exit burnup compared to the bundle shift is shown in Figure 4.3.

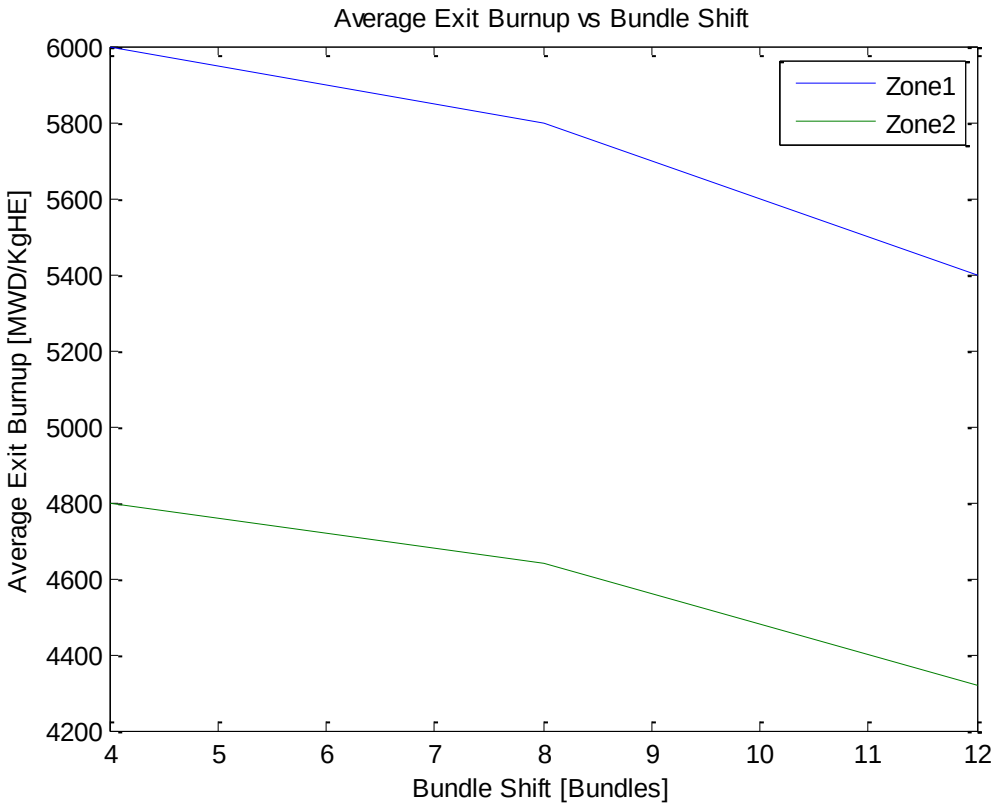

Figure 4.3. Average Exit Burnup vs Bundle Shift

As shown in Figure 4.3, a reduction in the number of bundles per refueling procedure increases the average exit burnup.

It is important to ensure that the betas are similar to that of the CANDU reactor to ensure that shut down procedures are effective for the new fuel type. These values are primarily determined by the isotopes being fissioned. The delayed neutron fraction in each precursor group l for each isotope j can be determined by the following equation:

$$\beta_{l,j} = \frac{\int_0^\infty dE \upsilon_{l,j}^D(\vec{r},E)\Sigma_{\mathrm{f,j}}(\vec{r},E)\phi(\vec{r},E)}{\int_0^\infty dE \upsilon_j^{ss}(\vec{r},E)\Sigma_{\mathrm{f,j}}(\vec{r},E)\phi(\vec{r},E)} = \frac{\sum_g \upsilon \sum_{f,l,j}^{D,g}(\vec{r})\,\phi^g(\vec{r})}{\sum_g \upsilon \sum_{f,j}^{g}(\vec{r})\,\phi^g(\vec{r})} \tag{4.1}$$

Which leads to;

$$\beta_l = \frac{\sum_j \beta_{l,j} \sum_g \upsilon \sum_{f,j}^{g}(\vec{r})\phi^g(\vec{r})}{\sum_j \sum_g \upsilon \sum_{f,j}^{g}(\vec{r})\phi^g(\vec{r})} \tag{4.2}$$

The isotopic depletion and betas for the CANDU and a fuel selection of 1% are shown in Figure 4.4 and Figure 4.5.

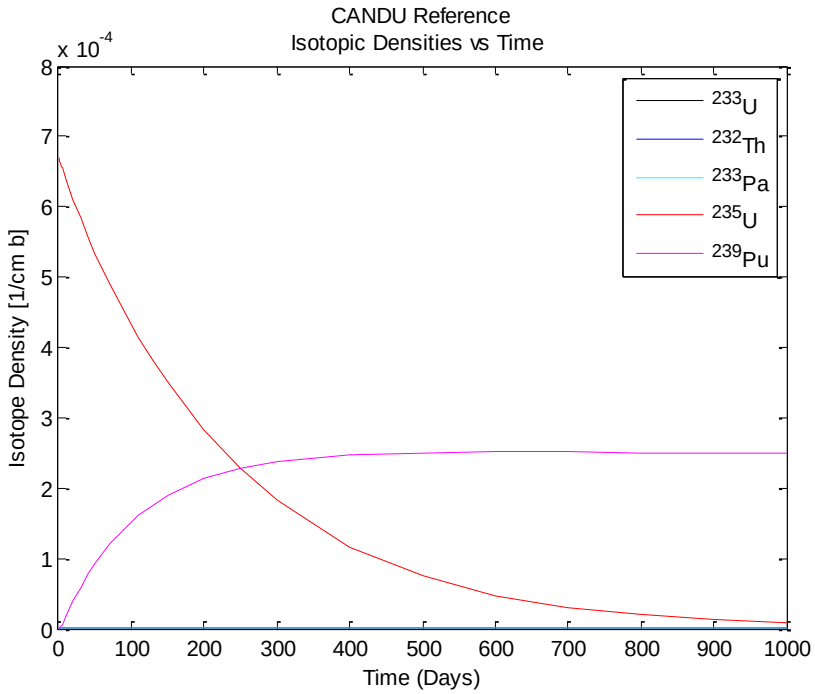

Figure 4.4. Reference Isotopic Densities.

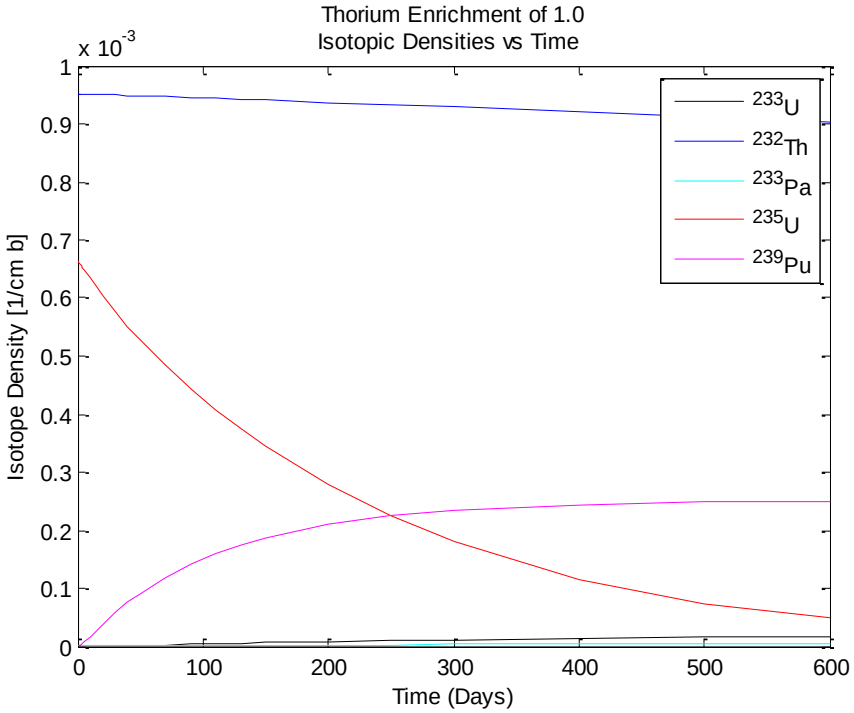

Figure 4.5. 1% Thorium Enriched Isotopic Densities.

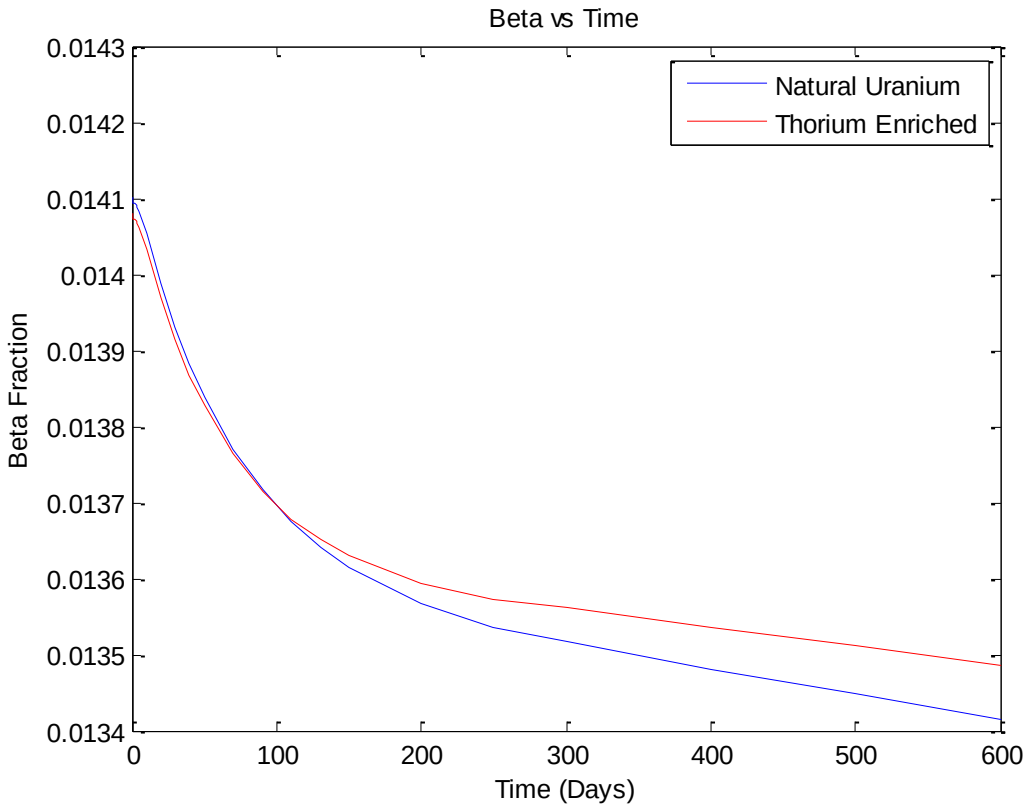

Figure 4.6. Delayed Neutron Fraction Comparison.

There is no significant change in the betas or isotopic depletion of the new fuel compared to the CANDU reactor. In the isotopic depletion graphs, the curves for each element closely resemble each other with the exception of thorium-232 which is not present in the CANDU core. The betas with respect to time also closely resemble one another. This is due to the minor quantities of thorium added to the fuel. The contributing isotopes to the beta fraction are U-233, U-235, and Pu-239. U-233 is only applicable in the case where the fuel is thorium enriched. The production of U-233, in combination with the new production, burnup, and decay of the other relevant isotopes creates a difference in the betas as shown in Figure 4.6.

Chapter 5. THE AUTOMATED REFUELING PROGRAM

The automated refueling program was developed in full for this project and is a set of procedures with the purpose of taking instantaneous and time-averaged data and performing channel refuelling as needed on the CANDU reactor. The core starts as an average of several random distributions of time averaged data. From there, the core is decayed and refueled as per scripts that analyze the parameters of the core in reference to the TA case and selected limits. Channels are carefully selected based on a set of predefined and dynamic rules in order to find a successful channel refueling procedure for that day. Once reactivity requirements are met, the core is simulated to decay for a Full Power Day (FPD) for the process to start once again. The exact procedures are outlined in the sections below.

5.1 Procedural Process

The process in which the procedures are performed is important for ensuring that the channels are refueled when required and the core is allowed to decay when the net core reactivity is positive. The top level procedure, named Master, is written in bash and is a managerial program dictating calls to other scripts and the transfer of data files. DONJON 4 is capable of writing ASCII files containing the data structures needed for analysis. These data structures are imported and analyzed by MATLAB scripts named; channel_select, channel_0FPD, and channel_check. The channel_select script is responsible for selecting the most eligible channel. channel_0FPD analyzes an instantaneous refueling of that channel and determines the reactivity added as well as if there are any rule breaches for the selected channel. The channel_check script analyzes the cumulative refueling procedures and determines when to proceed to the next day, as well as checks the core against the safety and procedural standards. Two DONJON scripts are used to perform instantaneous and one full power day refueling and decay procedures. The instantaneous script, 0FPD, refuels the selected channel after the channel_select script completed. 1FPD, is run once all the channels have been selected for that day. It refuels each channel from the previous day's decay and then decays for 1 FPD.

The logical process of the channel refueling procedure and the program schematics are shown in Figure 5.1 and Figure 5.2. The first step is to run TA and a set of averaged random instantaneous "age" distributions of that TA model. This snapshot is the day 0 core data from

which CANFUEL will begin. The program then selects the best channels to be refueled and prioritizes them accordingly based on predetermined selection criteria. Then, channels are selected and refueled sequentially until reactivity requirements are met. A failure in this process results in the elimination of those channels from the final selection. Success results in a 1 FPD decay of the core and a progression into the next step where the process starts again. This process is repeated until the required number of days has been completed.

In Figure 5.2, the squared edges represent modules executed in MATLAB; the rounded edges represent modules executed in DONJON; and the combination of rounded and squared edges, along with the data transfer between modules not shown in this figure, is executed in sh.

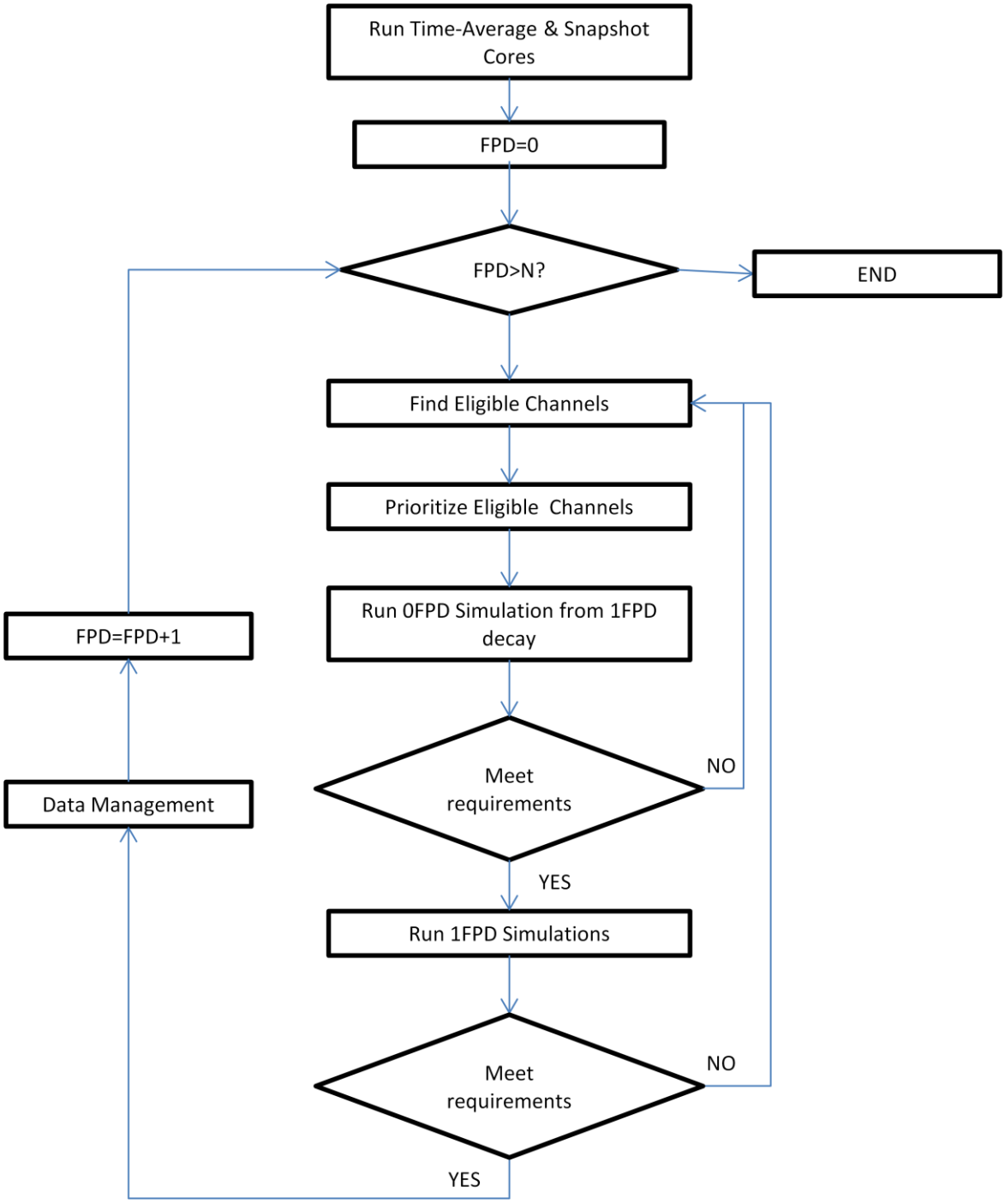

Figure 5.1. Channel Refueling Procedure

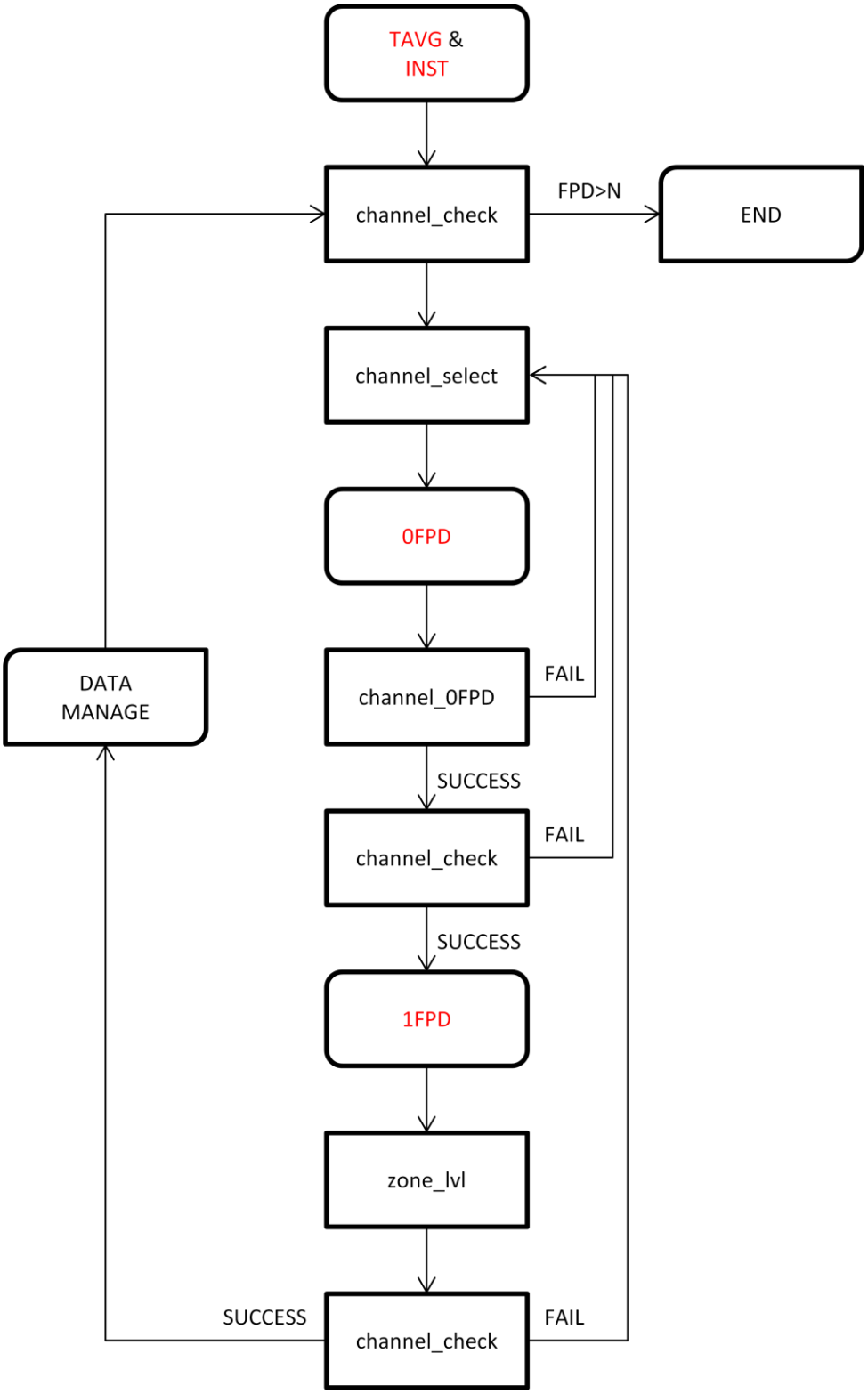

Figure 5.2. Refueling Script Procedure

5.2 Channel Elimination

The channel selection process determines which channel is most eligible for refueling based on a specific set of parameters. Each channel is tested and either eliminated or elected. A total of 100 of the most eligible channels are available as candidates.

The first set of constraints is based upon channel and bundle powers. The limits on channel and bundle power is 7300 kW and 935 kW respectively [11,18]. An initial set point of 6900 kW and 850 kW is used to eliminate channels which contain power levels greater than that specified. Rippled channel power, stated as the Channel Power Peaking Factor (CPPF) as described in equation 5.1, cannot exceed 1.10. Burnup constraints are also important for fuel economy and matching TA exit burnups. Any channel that falls below the TA exit burnup is also eliminated. Bundle and channel power and burnup information are retrieved from DONJON data files generated in the POWER data structure.

$$CPPF = \max\left[\frac{CP_{instantaneous}(m)}{CP_{TA}(m)}\right], \qquad m = channel\ number \tag{5.1}$$

Alternative elimination constraints are such that if required zone reactivity becomes positive due to refueling, further refuelling in that zone is prohibited. If the channel has been refueled within the last two days; that channel and the surrounding 8 channels are eliminated from selection. Once these restraints have been applied, the remaining channels are all still eligible for refueling. The goal is to have one hundred of the most eligible channels remaining and so the restraints are either relaxed or tightened depending on how many channels are remaining.

5.3 Channel Refinement

Channels selections are tallied in order to select the most eligible channels. This is done first by eliminating ineligible channels and then refining the constraints mentioned in the previous section as shown in Table 5.1. This process depends on the number of channels selected initially. The parameter refinement is shown in the table below. The constraints are adjusted until 100 of the best channels are selected.

Table 5.1. Channel selection constraints.

Constraints	Values	Increment
Maximum channel power	6900 kW	1.0%
Maximum bundle power	850 kW	1.0%
Rippled channel power over TA channel power	1.05	1.0%
Channel burnup compared to TA	70%	1.0%
Last refuel date	2 days	0.1 day

5.4 Channel Selection

Channel selection is performed on eligible channels based on three sets of priority. The first priority relies on the required reactivity of the channel. The channels are divided into their respective zones and measured against TA values to determine the required reactivity. This is determined by [19,20]:

$$\Delta\rho_i = \Delta\rho_c + \Delta\rho_{zcu}(z_i - z_{i0}) \tag{5.2}$$

where

$\Delta\rho_i$= the reactivity requirement of zone *i*

$\Delta\rho_c$= the core reactivity decay following a FPD decay divided by the number of zones

$\Delta\rho_{zcu}$= the reactivity worth of the zone controller

z_i= the current ZCU level

z_{i0}= the TA ZCU level

To determine the LZC fill for each zonal controller the snapshot model is compared to the TA model since this is the reference to which we try to obtain during the simulations. Zones are

initially set to 50% full with accordance to the TA model. From there they are incrementally filled according to the following equations:

$$\Delta Z_i = \alpha_i \left(k_{eff}(current) - k_{eff}(reference) \right) \tag{5.3}$$

$$\Delta Z_i = \alpha'_i \left(\frac{\phi_i}{\phi_{i,ref}} - \left\langle \frac{\phi}{\phi_{ref}} \right\rangle \right) \tag{5.4}$$

where

$\left\langle \frac{\phi}{\phi_{ref}} \right\rangle = \frac{1}{N} \sum_{i=1}^{N} \frac{\phi_i}{\phi_{i,ref}}$

α_i and α'_i = the maneuvering constant (120 and 2 respectively)

ϕ_i = the average instantaneous flux

N = the number of zones

The zone with the highest reactivity requirement is given first priority. The second priority is given to channels that have been selected the most during the channel refinement selection. If a channel continuously meets the constraints it is more eligible than channels that fail to do so. The final priority is given to channels with the highest burnup. The most eligible channel is then selected. Once a channel is selected and has passed all checks, channels within √10 channels are eliminated as shown in the Figure below, from being selected in the same day. The selection process must continue until the adjusted reactivity requirement is satisfied.

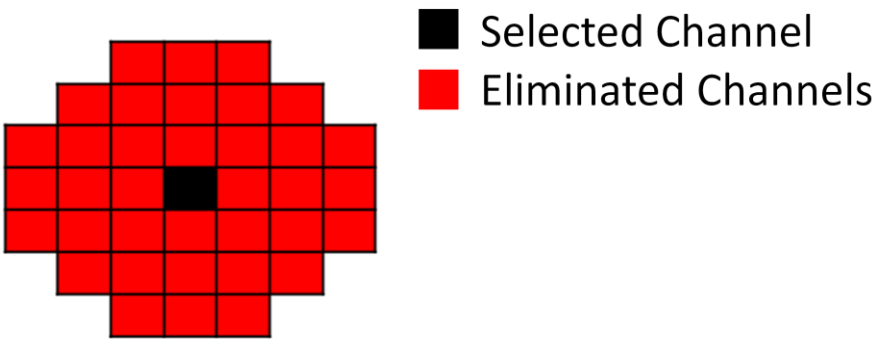

Figure 5.3 Eliminated Channels After a Successful Channel Selection.

5.5 Selection Check

Once a channel has been selected, 0FPD calculations are performed. The core must be analyzed to determine if further refuelling is necessary. The decision is based on the adjusted reactivity requirement. This is given in the equation below:

$$\Delta\rho'_i = \Delta\rho_i + \Delta\rho_{ij} \tag{5.5}$$

where $\Delta\rho_{ij}$ is the reactivity insertion to zone i due to a refueling of channel j. The zone reactivity requirement is a negative quantity while the reactivity insertion upon refueling is positive. If the adjusted zone reactivity requirement becomes positive, the candidates in that zone are eliminated from the final selection. Additional elimination set-points include; the channel must not provide a net positive reactivity to the reactor, the CPPF of the surrounding $\sqrt{10}$ channels after the prediction equation is applied must not exceed 1.10, and the refueled channel must not push a LZC beyond its limits.

Once the total adjusted required reactivity exceeds the original total required reactivity, the selection process is complete and the core is allowed to decay for 1 FPD. The results are then tested against the maximum allowed safety constraints for the reactor. If all criteria are met, the selection process continues. If one of the restraints is breached, the program steps back a FPD. The previously selected channels for that day are eliminated from re-selection and new channels are selected for that day to try and create a successful day of simulations.

5.6 Simulating for 100 Days

CANFUEL simulated a total of 100 days, over three months worth of reactor operations. While not optimized, the simulation provides a reasonable fuel selection for each day while maintaining the reactor within operational standards as required for a CANDU reactor. The channel and bundle powers were kept under the maximum values, with the largest values for both occurring on day 0, which was the random distribution snapshot. The maximum channel and bundle power for each day, as well as the burnup, refueling rate, and average zone level data are shown in Figure 5.4-5.5 and Table 5.2.

During the first few days of refueling, the program selected and refueled well above the average number of refueling channels. The reason for this is to compensate for the relatively high

average exit burnup of the channels in the core. The average of the average exit burnup for each channel is 4675 and 3721 MWd/t for burn zones one and two respectively. A diagram showing the burnzones is found in Annex 1. The minimum average exit burnup is 3680 and 3677 MWd/t. The average of the average exit burnup corresponds to roughly 70% of the average exit burnup of the TAV case. Subsequently, the program is forced to refuel an average of 10 channels per day during the first few days before it maintains an average refuel rate of 2.54 channels per day, which is much closer to the 2.27 channels per day given in the TA case.

The average zone level during the first 20 days drops to maintain criticality in the core due to the relatively high burnup of the core. After day 20, the average of the zone levels moves towards 0.50 which is to be expected for a reactor in a nominal operating state. Due to the high number of channels being refueled during the first 10 days of operations, 100 eligible channels were required in order to achieve the refueling rate.

While the maximum channel and bundle powers are close to the simulation limits, the average of the maximums for both are 7125 kW and 891 kW respectively. Although it may appear as though there is a pattern with the fluctuations of maximum channel and bundle powers, there is no such pattern. The position of each maximum point is at a different location for each day.

The power could be reduced if the program was optimized and acceptable limits were reset to below the simulation limits. Optimization would include weighting the average exit burnup at a much higher tally weight. This would emphasize channels with high burnup and would add significantly more reactivity to the core per refueling. With this in mind, fewer channels per day would need to be selected to reach the reactivity requirements of that day and higher exit burnups would be achieved throughout the program.

The maximum CPPF of the core is reasonable at 1.07. The average zone level for each day stays around 0.50, which indicates that the number of refuelings adequately introduces enough reactivity into the core without significant compensation from the LZCs.

Channel selection weighs each of the criteria evenly which is not optimized. This leads to a selection of some fuel channels that have a relatively low average exit burnup when compared to the TA state. This also leads to more refueling operations required to compensate for the reactivity because the reactivity insertion due to a higher burnup channel being refueled is larger

than one which has a relatively low average exit burnup as shown in Figure 4.1. For future versions of this code, the average exit burnup of the channel should hold a much higher weighting value during fuel selection.

Table 5.2. Simulation results compared to the TA reference.

	Time-Average	**Simulation**
Maximum channel power (kW)	7244	7296
Maximum bundle power (kW)	905	926
Rippled channel power over TA channel power	1.00	1.07
Average Zone Level	0.500	0.482
Refueling Rate (channels per day)	2.27	4.08
Exit Burnup in Zone 1 (MWd/t)	6700	5565
Exit Burnup in Zone 2 (MWd/t)	5360	4095

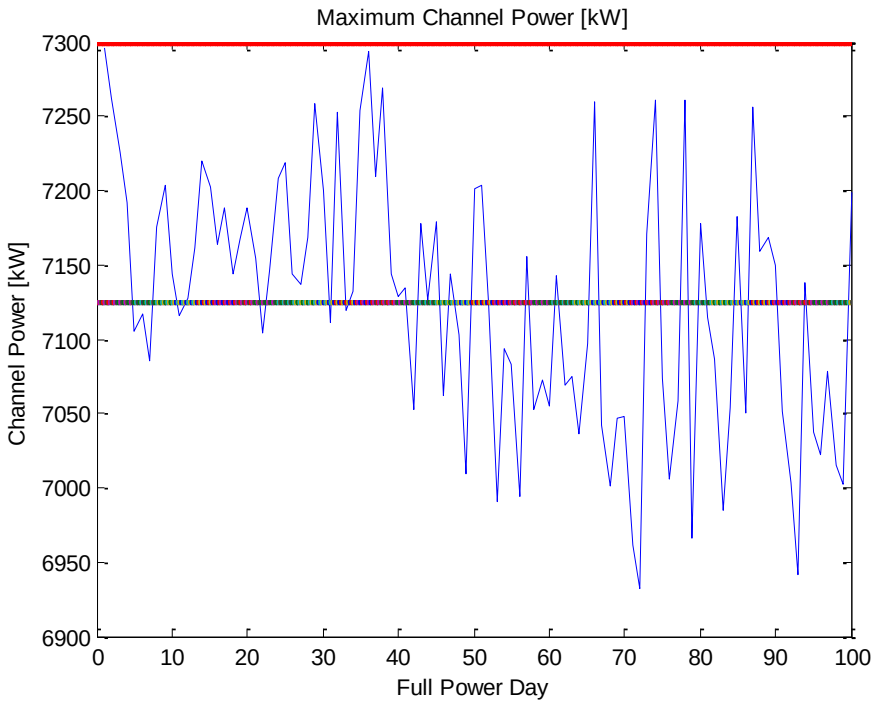

Figure 5.4 Maximum channel power results.

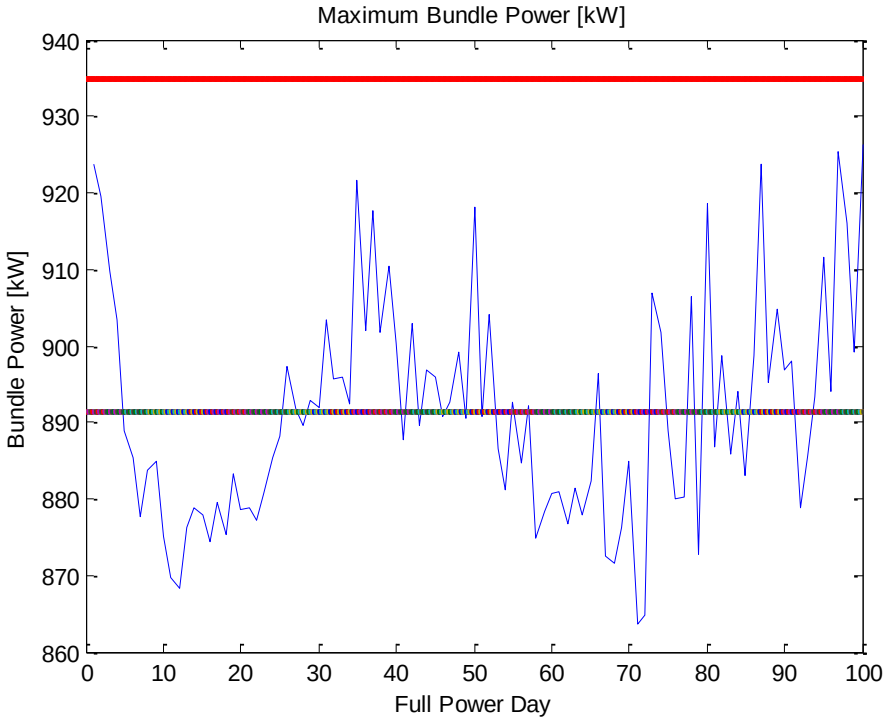

Figure 5.5 Maximum bundle power results.

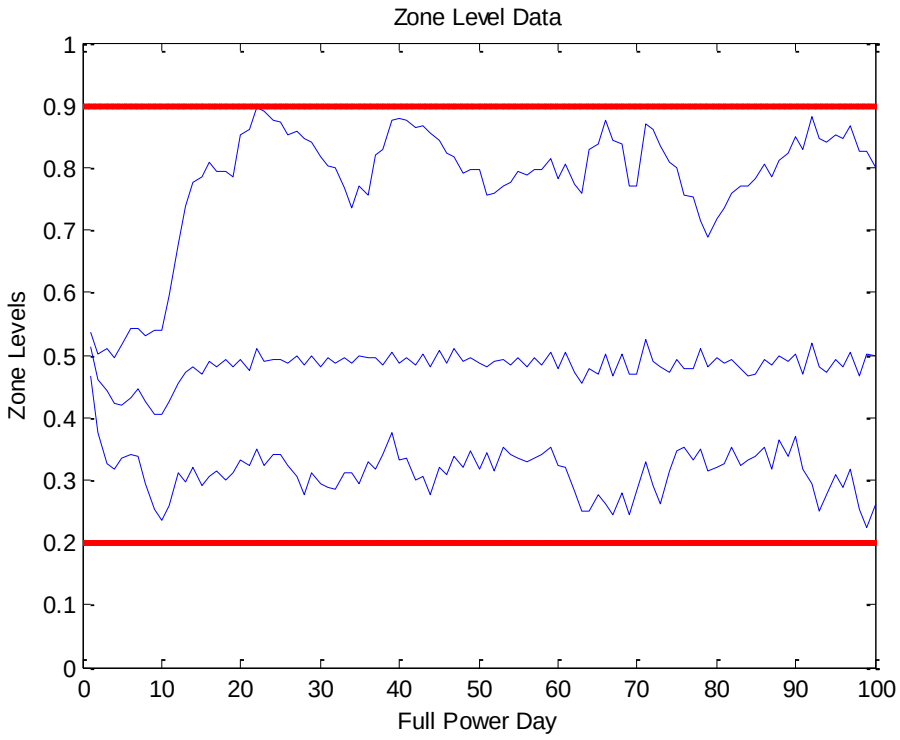

Figure 5.6 Maximum, minimum and average zone levels.

Chapter 6. **REACTIVITY INDUCED ACCIDENT**

It is important to determine the response of a reactivity insertion event within the core with a comparison to the nominal case. This event may be brought about by a number of events that are not relevant to this study. For the purposes of this paper, the accident will be simulated at hot full power (HFP) with the rod removal simulated using linear reactivity insertion up to the rod worth over a time-span of 0.1 seconds. The event will be tested in two situations. A critical random snapshot of a typical CANDU core for reference and a critical random snapshot of thorium enriched core.

For the case presented in this Section, the assumption that the rod is removed in 0.1 seconds is to simplify the case into a reactivity insertion exercise. It is important to determine the response in comparison to the nominal CANDU reactor in order to determine the feasibility of the new fuel choice.

6.1 Rod 11 Removal

To evaluate the core response to a rod 11 removal occurring within 0.1 seconds, a full core simulation using DONJON and TRIVAC was required. A 0.1 second removal time was chosen to limit the time effects of reactivity insertion and eliminate that variable from the analysis.

The process for creating the required starting point is described in Chapter 3. . From this point a random distribution of the TA core was set at an operating power of 2.061 MW. Zone levels are set to 50% full and the control rods are fully inserted into the core. Control rods are inserted vertically from the top of the core throughout the reactor. Rod 11 is located at the center of the core as shown in Figure 6.1.

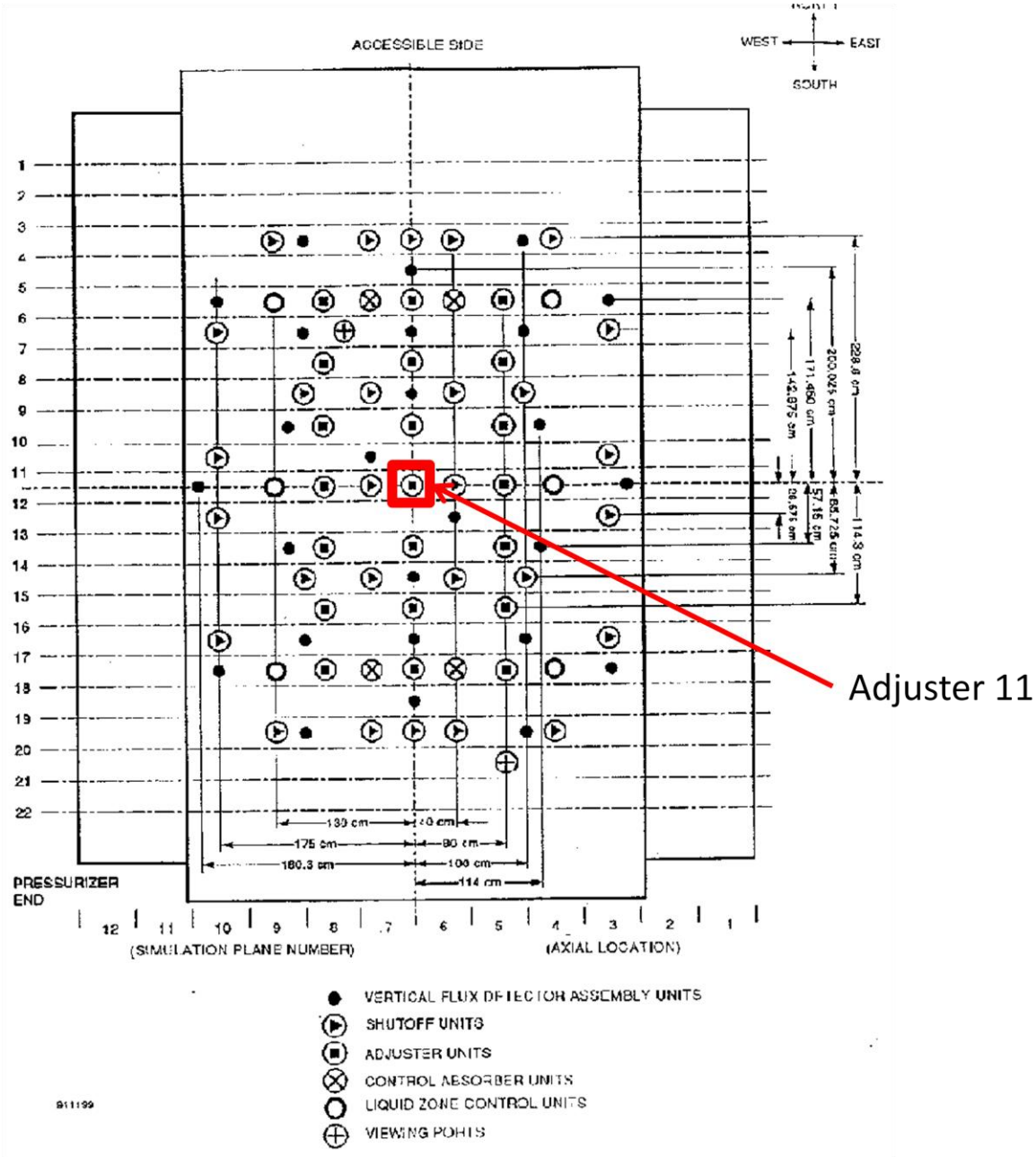

Figure 6.1 Adjuster Rod 11 Position in the Reactor

The initial kinetics parameters are obtained using the INIKIN: module of the TRIVAC computer code. The initial precursor concentrations are obtained as:

$$c_l(r,t_0) = \frac{1}{\lambda_l}\sum_{h=1}^{G} \upsilon\Sigma_{\mathrm{f,l,h}}^{\mathrm{del}}(\mathrm{r})\phi_{\mathrm{h}}(r,t_0); \qquad l = 1, N_d \tag{6.1}$$

where $\upsilon\Sigma_{f,l,h}^{del}(r)$ is υ times the delayed macroscopic fission cross section in energy group h for precursor group l, for each fissile isotope. The lambdas are given for eight groups in Table 6.1.

Table 6.1. Lambda Values.

Group	**Lambda (s^{-1})**
1	1.24666998E-02
2	2.82917004E-02
3	4.25244011E-02
4	1.33041993E-01
5	2.92467207E-01
6	6.66487694E-01
7	1.63478100E+00
8	3.55460000E+00

The rod removal started from the initial steady state conditions and was removed over a period of 0.1 seconds. The reactivity insertion due to the removal of rod 11 is 1.24 mk. The sufficiently small time increment allows a linear addition of reactivity into the core as opposed to the typical S-curve reactivity insertion due to rod removal. The KINSOL: module is then utilized to solve the space-time neutron kinetics equations at each step of the transient up to 3 seconds after the accident occurred. The Crank Nicholson temporal scheme was used to obtain the space-time kinetics solutions with a time step of 0.05 seconds. 0.05 seconds was chosen to adequately model the reactor power change.

The total reactor power of each simulation is provided in a case where there is no intervention through RRS and the activation of SDS1 or SDS2. The reactor power evolution for

each event is shown in Figure 6.2. The simulation starts with a prompt neutron jump, rapidly increasing the total reactor power. After roughly, 0.6 seconds, the prompt jump is over and the power increases at a smaller rate along the asymptotic period of $\frac{1}{\omega_1}$ of the inhour equation. Any fluctuations shown in Figure 6.2 are artifacts caused by the use of the Crank Nicholson finite difference temporal scheme. The power increase for both scenarios is very similar and no significant differences are shown throughout the evolution of the event.

The reactor flux is affected by the rod removal. Specific changes are detailed in Figure 6.3. The channel power increase is more significantly affected by the removal compared in the regions where the rod was. With the reactivity insertion in this area, it should be expected that the flux would increase to reflect that.

The evolution of the reactivity insertion event, while simplified, is a good indicator that the addition of thorium into the reactor has no significant impact on power evolution compared to the CANDU nominal case. Power increases and flux changes in the core show no unexpected variations and are very similar to that of the CANDU nominal case.

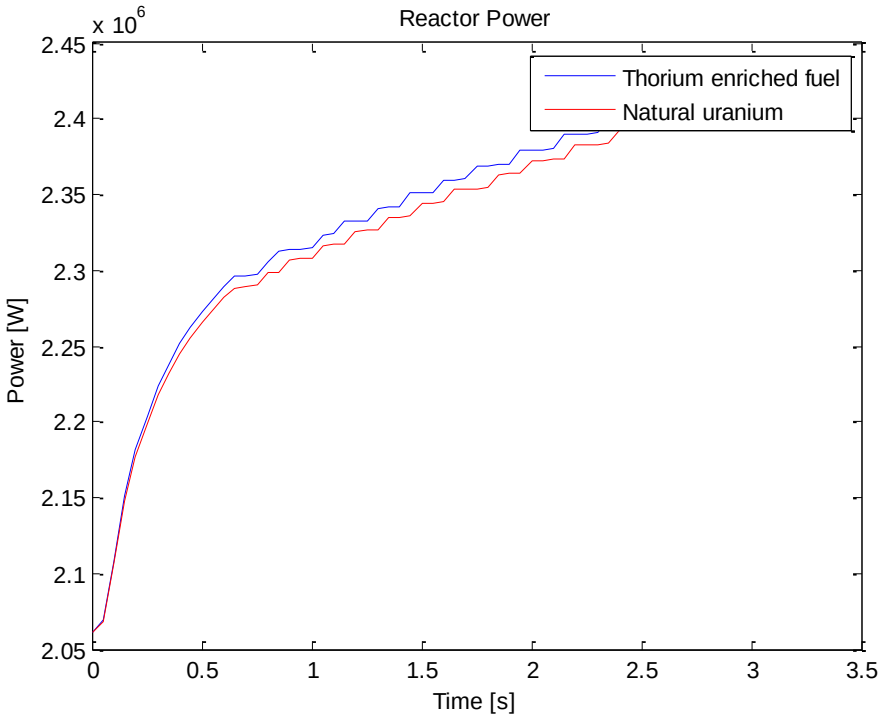

Figure 6.2 Reactor power after a rod removal event.

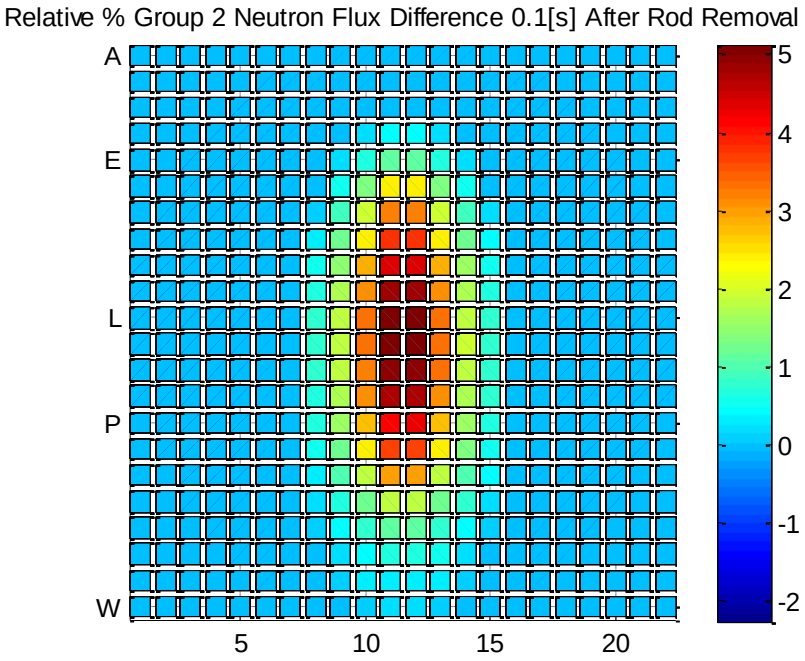

Figure 6.3 Relative % Group 2 Neutron Flux Difference 0.1s After Rod Removal.

CONCLUSION

A study into the effects of adding thorium into the CANDU core has been explored in this document. Guided by some background in reactor physics, the process of selection, data generation, and simulating refueling procedures has been documented, analyzed, and in some cases, validated. For further study, a simple reactivity insertion event was provided to compare to the nominal CANDU core and the results were discussed.

After introducing the concepts and equations used to model and study nuclear reactor physics, models were set up using the computer codes DRAGON, DONJON, and SERPENT. With these codes, the 2-dimensional lattice cell of a CANDU fuel bundle was created and studied with the inclusion of thorium into the fuel. Reactivity devices were then modeled in a 3-dimensional case in order to find the incremental cross-sections of the devices for the fuel composition within the lattice. These results were used to model the CANDU core in both Time-Average and Instantaneous simulations. 2-dimensional lattice calculations were then validated using Monte-Carlo calculations performed in SERPENT. This data was essential for selecting a fuel composition.

With the constraints determined, several objectives for the new fuel were selected to choose an operational fuel. Such objectives included the quantity of thorium included in the fuel, burnup, reactivity insertion, bundle refueling patterns, isotopic contents, and delayed neutron fraction compared to natural uranium. Finally, a 1% enrichment of thorium in the fuel was decided upon.

With the device and fuel data generated, an automated refueling program was executed to determine the feasibility of the fuel selection. By setting dynamic constraints on the instantaneous snap-shot of the reactor, fuel channels were selected to keep the reactor operating within safety and reactivity objectives. The process involved selecting channels based on the elimination of ineligible channels and selection refinement to determine a small set of ideal candidates. Once the reactivity requirements for the day were satisfied, the core was allowed to decay for a period of one full power day. The new snap-shot was then analyzed to determine the success of the previous channel selection(s), and to determine new selection(s) for the day.

The simulated a period of 100 days of continuous operations. Maximum channel and bundle powers were 7296 kW and 926 kW respectively and were very close to the Time-Average

results. The Channel Power Peaking Factor was 1.07 which is acceptable for the CANDU reactor. The average fill of Liquid Zone Controllers was 0.48 indicating that refueling operations were adequate in maintaining core reactivity. A refueling rate of roughly 4 bundles per day, about 1.5 more bundles than the Time-Average case and an average exit burnup of about 70% of the Time-Average value indicate that the selection process needs to be optimized further. Optimization would include weighting the average exit burnup at a higher priority selection parameter by increasing the weight of each selection tally. This would increase the reactivity insertion of each refueling and reduce the refueling rate in the core and allow higher exit burnups.

A rod removal scenario was studied to determine the relation to natural uranium. The rod was removed in a period of 0.1 seconds. This was to limit and simplify the variables and to determine the response between thorium enriched and natural uranium cores. The power response, with no intervention from safety devices over a 3 second time frame was very similar for both cases. The change in group 2 flux was greatest in the channels that were near the rod removal. The new fuel selection was deemed acceptable for these purposes.

Future work that should be considered is the optimization of the program to improve fuel selection and simulate a core that more resembles the Time Average case. A fuel selection which increases the average exit burnup of the core would produce longer residence times of the fuel and would reduce the number of refuelings required. This would further test the feasibility of thorium as a fuel and make it a more desirable fuel source for the CANDU reactor.

BIBLIOGRAPHY

[1] World Nuclear Association, "Uranium Markets: World Nuclear Association," September 2008. [Online]. Available: http://www.world-nuclear.org/info/inf22.html. [Accessed 06 December 2009].

[2] World Nuclear Association, "Canadian Uranium Production," October 2009. [Online]. Available: http://www.world-nuclear.org/info/inf49.html. [Accessed 06 December 2009].

[3] Nuclear Power Technology Development Section, Thorium Fuel Utilization, Vienna: IAEA, 2002.

[4] P. Boczar, Xie Zhonsheng, CANDU Fuel-cycle Vision, Chalk River: AECL, 1998.

[5] A. Hebert, R. Roy, G. Marleau, "A User Guide for DRAGON Version4," Ecole Polytechnique de Montreal, Montreal, 2011.

[6] A. Hebert, R. Chambon, D. Sekki, "A User Guide for DONJON Version4," Ecole Polytechnique de Montreal, Montreal, 2011.

[7] J. Leppänen, "PSG2 / Serpent – a Continuous-energy Monte Carlo Reactor Physics Burnup Calculation Code," VTT Technical Research Centre of Finland., 2011.

[8] A. Hebert, Applied Reactor Physics, Montreal: Presses internationales Polytechnique, 2009.

[9] D. Rozon, Introduction to Nuclear Reactor Kinetics, Montreal, 1998.

[10] A. Santamarina, D. Bernard, Y. Rugama, "JEFF-3.1.1 evaluated data library," Nuclear Energy Agency, Paris, 2009.

[11] B. Rouben, "CANDU Fuel-Management Course," CANTEACH, 1999. [Online]. Available: http://canteach.candu.org/library/20031101.pdf . [Accessed 15 01 2010].

[12] CANDU Energy Inc., "Enhanced CANDU 6 Technical Summary," CANDU Energy Inc., Mississauga, 2012.

[13] M. Dahmani, G. Marleau, R. Le Tellier, "Modelling Reactivity Devices for Advanced CANDU Reactors Using the Code DRAGON," Annals of Nuclear Energy (Elsevier), 2007.

[14] R. Roy, G. Marleau, J. Tajmouati, D. Rozon, "Modeling of CANDU Reactivity Control Devices with the Lattice Code DRAGON," Institut de Genie Energetique, Ecole Polytechnique de Montreal, Montreal, Quebec, 1993.

[15] C. Jeong, H. Choi, "Compatibility Analysis on Existing Reactivity Devices in CANDU 6 Reactors for DUPIC Fuel Cycle," *Nuclear Science and Engineering*, vol. 134, pp. 265-280, 1999.

[16] G. Marleau, E. Varin, "CANDU reactor core simulations using fully coupled DRAGON and DONJON calculations," *Annals of Nuclear Energy*, p. 682–691, 2006.

[17] F. Brown, "“K-effective of the World” and Other Concerns for Monte Carlo Eigenvalue Calculations," *Progress in Nuclear Science and Technology*, vol. 2, pp. 738-742, 2011.

[18] S. Zhang, B. Rouben, X. Jiaotong, "CANDU Fuel Management," CANTEACH, May 1999. [Online]. Available: https://canteach.candu.org/Content%20Library/20054411.pdf. [Accessed 03 06 2011].

[19] H. Choi, "A Fast-running Fuel Management Program for a CANDU Reactor," *Annals of Nuclear Energy*, vol. 27, pp. 1-10, 2000.

[20] H. Choi, "Automatic Refueling Simulation of a DUPIC Fuel Transition Core," *Annals of Nuclear Energy*, vol. 35, p. 1695–1700, 2008.

[21] B. Rouben, "CANDU Fuel Management Course," Atomic Energy of Canada Ltd., Deep River.

ANNEX 1 – CANDU Core Figures

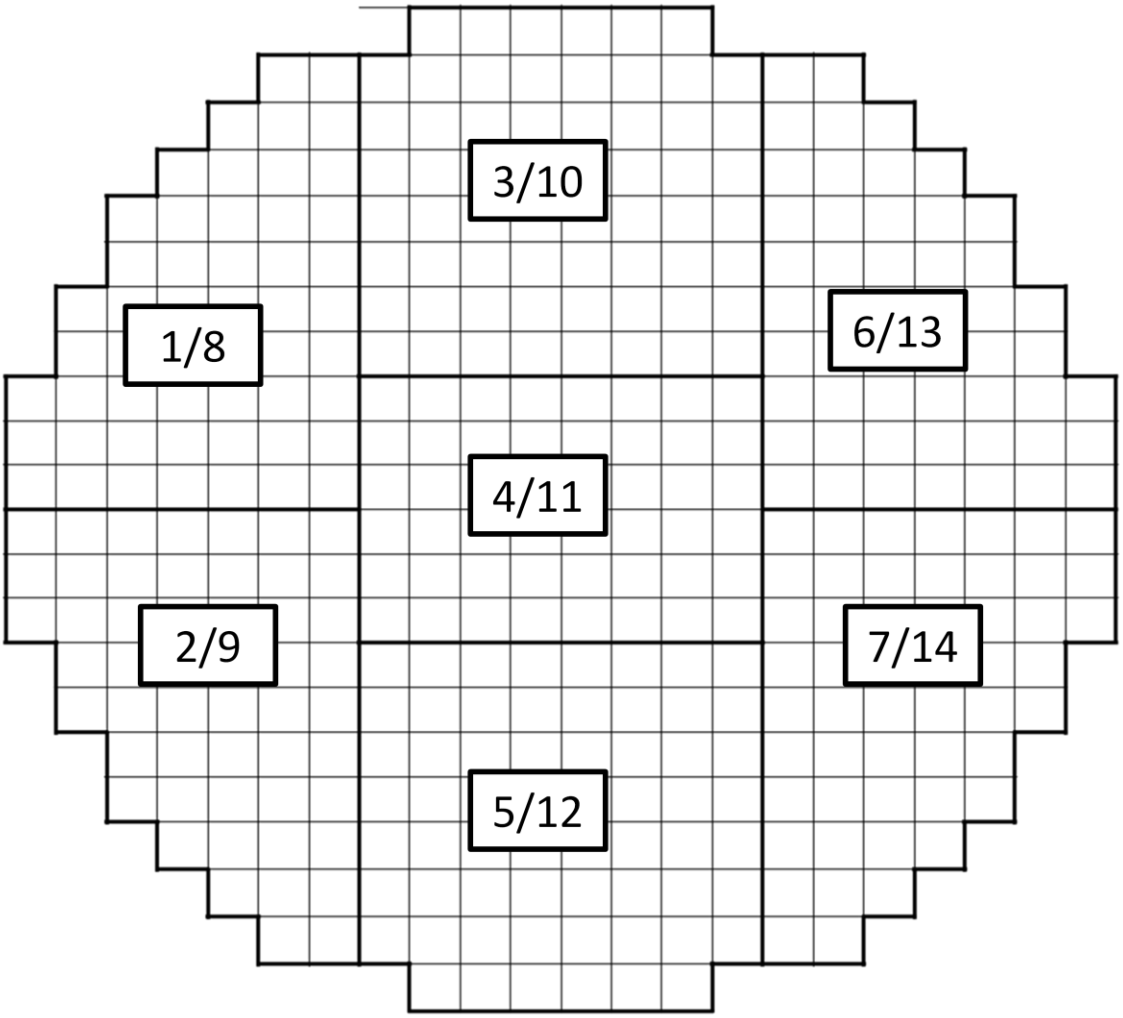

A.1.1 Zone discrimination for zone control 1 Zone discrimination for zone control using LZC.

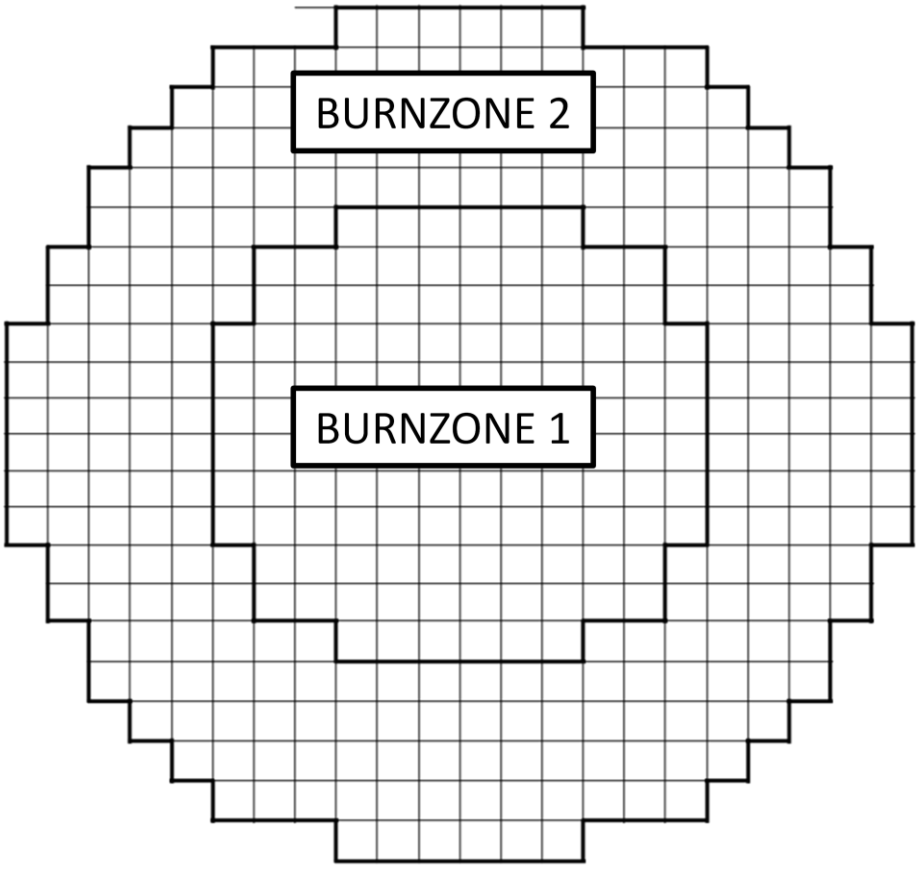

Table A1.2 Burnup zones 1

ANNEX 2 – Refueling Simulation Script

```
#!/bin/bash
#
# author      : B. Holmes
# description : This file is used to simulate a refueling strategy
#               for a CANDU-6 reactor through the utilization of the DONJON full
#               core reactor physics simulator with feedback from a set of MATLAB
#               scripts. Please ensure that all necessary files are present before
running.

###
# Directories & Variables:
###
# A list of all relevant directories
base=/home/Holmes/DONJON4/                          #Base directory for DONJON
base_CPO=/home/Holmes/DONJON4/Candu6_CPOs/          #Dragon CPO type databases
base_Data=/home/Holmes/DONJON4/Data/                #Donjon structure type databases
base_Rslt=/home/Holmes/DONJON4/Results/             #Donjon result type databases
base_Proc=/home/Holmes/DONJON4/procedures/          #Donjon procedures
base_FPD=/home/Holmes/DONJON4/FPD/                  #FPD data files for reference
base_Arch=/home/Holmes/DONJON4/Archive/             #Collection of time organized
databases
base_Plot=/home/Holmes/DONJON4/Archive/FigurePlots/  #Collection of time organized data
plots
script=/home/Holmes/Holmes_Code/MATLAB/             #MATLAB scripts
MATLAB=/c:/"Program Files"/MATLAB/R2010a/bin/       #MATLAB run directory

# A list of all relevant files
C6_INST=Candu6_INST_RAND.x2m                       #Random Donjon simulation
C6_1FPD=Candu6_INST_1FPD.x2m                       #1FPD time increment Donjon
simulation
C6_0FPD=Candu6_INST_0FPD.x2m                       #0FPD time increment Donjon
simulation
C6_TAVG=Candu6_TAVG.x2m                            #TAVG Donjon simulation
INST_RES=Candu6_INST_RAND.result                   #Random Donjon result
FPD_RES=Candu6_INST_1FPD.result                    #1FPD time increment Donjon result
FPD_RES0=Candu6_INST_0FPD.result                   #0FPD time increment Donjon result
TAVG_RES=Candu6_TAVG.result                        #TAVG Donjon result
select=channel_select                              #Channel selection script
check=channel_check                                #Channel checking script

# A list of all relevant variables
# Keff
# FPD
# FPD_Tot
# Chan
# Success
FPD=1
FPD_Tot=100
Success="false"
count=0

###
# Data management
###
cd $base_CPO
rm -f pmap
rm -f fmap
rm -f matex
rm -f mac
rm -f dvice
```

```
rm -f trak
rm -f geo
rm -f pmap_RAND
rm -f fmap_RAND
rm -f matex_RAND
rm -f mac_RAND
rm -f dvice_RAND
rm -f trak_RAND
rm -f geo_RAND
rm -f flux_RAND

cd $script
rm -f Keff.txt
rm -f ChSel.txt
rm -f Direction.txt
rm -f Success.txt
rm -f FPDRef.txt
rm -f SetZone.txt
rm -f SetRho.txt
rm -f SetRea.txt
rm -f AppRea.txt
rm -f zonesearch.txt
rm -f K_decay.txt
>Success.txt

cd $base_Proc
cp -f SetZone_50.c2m SetZone.c2m

###
# Run TAVG and RAND simulations
###
cd $base
#./rdonjon "$C6_TAVG"
./rdonjon "$C6_INST"
cd $base_Data
cp -f fmap   "$base_CPO"fmap
cp -f pmap   "$base_CPO"pmap
cp -f mac    "$base_CPO"mac
cp -f matex  "$base_CPO"matex
cp -f dvice  "$base_CPO"dvice
cp -f geo    "$base_CPO"geo
cp -f trak   "$base_CPO"trak

cd $script
echo "Adjust Zone Levels"
matlab -nodisplay -nosplash -nodesktop -r "zone_lvl; quit;"
sleep 30
cd $base
./rdonjon Candu6_INST_GPT.x2m
./rdonjon "$C6_0FPD"
cd $script
matlab -nodisplay -nosplash -nodesktop -r "channel_check; quit;" # >Success.txt
>>Keff.txt
sleep 40
Success="true"
Keff=`tail -1 Keff.txt`
Info=`cat Info.txt`
Chan="A01"
echo "$Chan $FPD $Info $Keff $Success " >> FPDRef.txt

###
# Initialize Keff & Success variables
###
```

```
cd $base_Rslt
grep ">|RESULTING" $INST_RES #Print starting K-Eff

while [ $FPD -le $FPD_Tot ]; do

	if [ $Success = "true" ]; then
		cd $script
		matlab -nodisplay -nosplash -nodesktop -r "channel_check; quit;"
		sleep 40
		Success=`cat Success.txt`
		Keff=`tail -1 Keff.txt`
	fi

	if [ $Success != "true" ]; then
		###
		# Select a Channel
		###
		cd $script
		echo "Select a channel for refueling"
		matlab -nodisplay -nosplash -nodesktop -r "channel_select; quit;"
		sleep 35
		Chan=`tail -1 ChSel.txt`
		echo "Eligible channel 0FPD run for channel $Chan"

		###
		# Run eligible channel
		####
		cd $base
		./rdonjon "$C6_0FPD"
		cd $script
		matlab -nodisplay -nosplash -nodesktop -r "channel_0FPD; quit;"
		sleep 45
		cp -f "$base_CPO"fmap   "$base_Data"fmap
		cp -f "$base_CPO"pmap   "$base_Data"pmap
		cp -f "$base_CPO"mac    "$base_Data"mac
		cp -f "$base_CPO"matex  "$base_Data"matex
		cp -f "$base_CPO"dvice  "$base_Data"dvice
		Success=`cat Success.txt`
		echo "Channel selection is a success? $Success"

		###
		# Update core info
		###
		Info=`cat "$script"Info.txt`
		Keff=`tail -1 "$script"Keff.txt`
		echo "$Chan $FPD $Info $Keff $Success " >> "$script"FPDRef.txt
	fi

	###
	# Check Simulation results
	###
	cd $script
	matlab -nodisplay -nosplash -nodesktop -r "channel_check; quit;" # >Success.txt
>>Keff.txt
	sleep 40
	Success=`cat Success.txt`
	Keff=`tail -1 Keff.txt`
	echo "Channel selection is a success? $Success"

	###
	# Run 1FPD and check if channel selection is complete
	###
	if [ $Success = "true" ]; then
```

```
            ###
            # Refuel channels in current day and check
            ###
            cd $script
            if [[ -s ChSel.txt ]]; then #Continue with last refueled channel in case
of 0 selections for the day
                  if [  $FPD -gt 0 ]; then
                        Chan=`tail -1 ChSel.txt`
                  fi
            fi
            ###
            # Run 1FPD Simulations
            ###
            cd $base
            ./rdonjon "$C6_1FPD"
            cd $script
            echo "1" > zonesearch.txt
            echo "Adjust Zone Levels"
            matlab -nodisplay -nosplash -nodesktop -r "zone_lvl; quit;"
            sleep 30

            ###
            #Update core info with zone levels
            ###
            cd $base_Data
            cp -f fmap   "$base_CPO"fmap
            cp -f pmap   "$base_CPO"pmap
            cp -f matex  "$base_CPO"matex
            cp -f dvice  "$base_CPO"dvice
            cd $base_Proc
            cp -f SetChan_empty.c2m SetChan.c2m
            cd $base
            ./rdonjon "$C6_0FPD"

            ###
            #Determine if successful refueling sequence
            ###
            cd $script
            matlab -nodisplay -nosplash -nodesktop -r "channel_check; quit;"
      sleep 40
            Success=`cat Success.txt`
            Keff=`tail -1 Keff.txt`
            echo "$Keff" > K_decay.txt
            if [ $Success != "false" ]; then
                  Success="true"
                  FPD=`expr $FPD + 1 `
                  echo "Increment FPD to $FPD"
                  fill="$Chan"
                  echo "New Keff is $Keff"
            else
                  Chan="$fill"
            fi
            Info=`cat Info.txt`
            echo "$Chan $FPD $Info $Keff $Success " >> FPDRef.txt
      fi

      ###
      # Data management
      ###
      # Condition 1: Refueling channel success
      if [ $Success = "true" ]; then
            if  [ $FPD != 0 ]; then
                  #to archive
```

```
                cd $base_Data
                cp -f fmap   "$base_Arch"fmap_"$FPD"
                cp -f pmap   "$base_Arch"pmap_"$FPD"
                cp -f matex  "$base_Arch"matex_"$FPD"
                cp -f dvice  "$base_Arch"dvice_"$FPD"
                cp -f mac    "$base_Arch"mac_"$FPD"
                cd $base_Rslt
                cp -f $FPD_RES  "$base_Arch""$FPD_RES"_"$FPD"
                cp -f $FPD_RES0 "$base_Arch""$FPD_RES0"_"$FPD"
                cp -f "$script"AppRea.txt "$base_Arch"AppRea_"$FPD"
                cp -f "$script"ChSel.txt "$base_Arch"ChSel_"$FPD"
                cp -f "$script"FPDRef.txt "$base_Arch"FPDRef.txt
                cp -f "$base_Proc"SetZone.c2m "$base_Arch"SetZone_"$FPD"
                if [[ ! -s ChSel.txt ]]; then
                      cd $base_Arch
                      > ChSel_"$FPD"
                fi

                #to reference
                cd $base_Data
                cp -f fmap         "$base_FPD"fmap
                cp -f pmap         "$base_FPD"pmap
                cp -f matex        "$base_FPD"matex
                cp -f dvice        "$base_FPD"dvice
                cp -f mac          "$base_FPD"mac
                cd $base_Proc
                cp -f SetZone.c2m  "$base_FPD"SetZone.c2m
                cd $script
                cp -f ChSel.txt    "$base_FPD"ChSel.txt
                cd $base_Rslt
                cp -f $FPD_RES     "$base_FPD"$FPD_RES
                cp -f $FPD_RES0    "$base_FPD"$FPD_RES0

                #to read
                cd $base_Data
                cp -f fmap   "$base_CPO"fmap
                cp -f pmap   "$base_CPO"pmap
                cp -f matex  "$base_CPO"matex
                cp -f dvice  "$base_CPO"dvice
                cp -f mac    "$base_CPO"mac

                #Perform LZC perturbations
                echo "Determine updated device reactivity worth"
                cd $base
                ./rdonjon Candu6_INST_GPT.x2m

                #delete files
                cd $script
                rm -f AppRea.txt
                rm -f Direction.txt
                rm -f ChEli.txt
                rm -f ChSel.txt
                rm -f no_ref.txt
                rm -f SetRea.txt
                rm -f SetRho.txt
                rm -f tal_ref.txt
                rm -f K_decay.txt
        fi

#Condition 2: Failure
elif [ $Success = "false" ]; then
        echo "Channel selection is invalid "
        echo "Restart simulation from last FPD "
```

```
                #Reset condition
                Success="true"
                Chan="$fill"

                #delete bad data
                cd $script
                rm -f AppRea.txt
                rm -f Direction.txt
                rm -f ChEli.txt
                rm -f ChSel.txt
                rm -f no_ref.txt
                rm -f SetRea.txt
                rm -f SetRho.txt
                rm -f tal_ref.txt

                #Iosalte Failed Zone Levels
                cd $base_Proc
                cp -f SetZone.c2m  SetZone_fail.c2m
                #import FPD data
                cd $base_FPD
                cp -f fmap   "$base_CPO"fmap
                cp -f pmap   "$base_CPO"pmap
                cp -f matex  "$base_CPO"matex
                cp -f dvice  "$base_CPO"dvice
                cp -f fmap   "$base_Data"fmap
                cp -f pmap   "$base_Data"pmap
                cp -f matex  "$base_Data"matex
                cp -f dvice  "$base_Data"dvice
                cp -f SetZone.c2m  "$base_Proc"SetZone.c2m
                cp -f $FPD_RES     "$base_Rslt"$FPD_RES
                cp -f $FPD_RES0    "$base_Rslt"$FPD_RES0

        #Condition 3: Failure due to low reactivity
        elif [ $Success = "fail1" ]; then
                echo "Channel selection is invalid due to low bulk reactivity"

        #Condition 4: Run eligible channels
        elif [ $Success = "fail0" ]; then
                echo "Channel 0FPD prediction loop failed"
                exit

        #Condition F: Failure due to program error
        else
                echo "Program has failed, please try again"
                exit
        fi
done

echo "Completion of refueling loop"
```

ANNEX 3 – Channel Selection for Day 53

The selection process starts with an execution of channel_check to determine the required reactivity of the core. In this case the required reactivity is slightly negative, as shown in table A3.1.

A3.1 Required Reactivity

Zone	Required Reactivity
1	2.93E-04
2	-7.06E-05
3	4.49E-04
4	-9.02E-04
5	-4.31E-04
6	-3.72E-04
7	1.28E-04
8	1.79E-04
9	4.38E-04
10	1.18E-04
11	3.56E-04
12	4.32E-04
13	-3.54E-04
14	-8.36E-04
Total	-5.73E-04

An execution of the channel_select script starts by eliminating ineligible channels. There are 43 channels eligible for refueling this day sorted by the total number of tallies received by each channel. These channels are stored in a data file for further use. An example of the highest tallied channels are shown in Table A3.2.

A3.2 Tally Sorted Channel Selection.

Channel Number	Channel Power	Bundle Power	Burnup	CPPF	First Priority	Second Priority	Tally Total	Burnup
371	17	9	34	9	0	0	69	4685.983
332	17	10	34	9	0	0	70	4531.453
369	17	9	34	10	0	0	70	4727.216
18	17	10	34	10	0	0	71	4521.854
365	17	10	34	10	0	0	71	4581.95

The selection is then refined based on priority, the axial refueling pattern, among others and is represented in Table A3.3.

A3.3 Final Channel Selection.

Channel Number	Channel Power	Bundle Power	Burnup	CPPF	First Priority	Second Priority	Tally Total	Burnup
249	7	5	34	12	0	1	58	6301.151
243	9	5	34	11	0	1	59	6273.476
203	10	6	34	10	0	1	60	6253.648
180	12	6	34	10	0	1	62	6239.333
138	9	5	34	14	0	1	62	6318.115
199	10	6	34	13	0	1	63	6293.779
176	9	5	34	15	0	1	63	6324.522
132	9	5	34	16	0	1	64	6352.299

The final selection is the channel listed at the bottom of this table. In this case, the channel is J08. Once the channel is selected, a 0FPD DONJON script is executed and the the success parameters and adjusted reactivity are examined in the channel_0FPD and channel_check scripts respectively. For this case, one channel was all that was required for refueling.

ANNEX 4 – Refueling Log

The table below represents the refueling log for each day and selection. True, indicates that the required fueling for the day has been completed and the program can move forward. Pass indicates that the fuel channel selection is acceptable but further refueling is required. Fail0 represents a channel selection that does not meet the guidelines. False, indicates that the channels selected for that day do not meet the guidelines once the program has progressed a FPD.

Channel	Day	Max Channel Power (kW)	Max Bundle Power (kW)	CPPF	Selection Outcome
A01	1	7296.01	923.66	0.98	TRUE
N12	1	7259.18	922.26	1.01	pass
N12	2	7262.07	919.63	1.01	TRUE
M11	2	7227.62	913.21	1.03	pass
C09	2	7226.59	913.99	1.01	pass
C14	2	7218.47	912.71	1.01	pass
R11	2	7222.49	912.59	1.01	pass
S15	2	7199.85	909.77	1.01	pass
Q18	2	7213.64	911.91	1.01	pass
R06	2	7262.95	916.92	1.01	pass
M02	2	7268.84	918.92	1.01	pass
U09	2	7229.83	913.76	1.01	fail0
N21	2	7214.62	912.09	1.01	pass
E18	2	7216.03	912.33	1.01	pass
E05	2	7237.56	915.62	1.01	pass
H03	2	7253.3	917.67	1.01	pass
H20	2	7212.8	911.91	1.01	pass
H20	3	7226.22	909.62	1.02	TRUE
L13	3	7171.15	904.06	1.03	pass
K21	3	7177.65	904.94	1.02	pass
D16	3	7178.68	905.16	1.02	pass
C06	3	7195.22	907.46	1.02	pass
K02	3	7225.12	911.86	1.02	pass
F03	3	7204.11	908.87	1.02	pass
F20	3	7182.76	905.6	1.02	pass
P20	3	7177.37	904.85	1.02	pass
L09	3	7214.83	909.37	1.03	pass
Q03	3	7213.95	909.18	1.02	pass
S08	3	7206.41	907.68	1.02	pass

S17	3	7181.76	905.37	1.02	pass
B12	3	7186.37	906.18	1.02	pass
U05	3	7196.23	907.2	1.02	fail0
T13	3	7185.07	905.64	1.02	pass
V10	3	7192.23	906.67	1.02	fail0
W10	3	7192.98	906.81	1.02	fail0
W09	3	7193.5	906.9	1.02	fail0
T13	3	7193.5	906.9	1.02	fail0
T13	4	7191.35	903.47	1.03	TRUE
O10	4	7164.76	899.75	1.03	pass
Q13	4	7136.2	896.07	1.03	pass
O02	4	7187.65	902.92	1.03	pass
U17	4	7152.26	898.7	1.03	pass
B16	4	7151.28	898.71	1.03	pass
T10	4	7156.06	898.85	1.03	pass
V13	4	7153.57	898.84	1.03	pass
R20	4	7148.33	898.21	1.03	pass
U06	4	7160.62	899.69	1.03	pass
A10	4	7155.08	899.22	1.03	pass
L15	4	7133.62	896.9	1.04	pass
S03	4	7165.04	900.16	1.03	pass
J09	4	7171.75	901.68	1.03	pass
G18	4	7135.94	896.74	1.03	pass
G05	4	7176.83	902.98	1.03	pass
H13	4	7131.92	896.09	1.03	pass
H13	5	7105.18	888.81	1.04	TRUE
O14	5	7071.24	884.5	1.04	pass
C18	5	7093.19	887.63	1.03	pass
T19	5	7094.67	887.74	1.03	pass
K17	5	7114.25	891.55	1.04	pass
O18	5	7152.28	893.29	1.03	pass
A14	5	7095.36	887.92	1.03	pass
P05	5	7178.83	897.46	1.03	pass
T04	5	7104.88	888.87	1.03	pass
K06	5	7169.58	898.56	1.03	pass
N08	5	7140.45	891.96	1.04	pass
E07	5	7104.7	889.74	1.03	pass
K11	5	7093.35	887.34	1.06	pass
U08	5	7101.23	888.41	1.03	pass
U15	5	7091.65	887.25	1.03	pass
F12	5	7076.55	886.09	1.04	pass
F12	6	7117.52	885.39	1.05	TRUE
H07	6	7145.36	890.74	1.05	pass

H16	6	7121.02	884.94	1.05	pass
K19	6	7125.31	897.41	1.04	pass
O16	6	7125.03	885.53	1.04	pass
H11	6	7090.8	883.68	1.05	pass
M06	6	7207.45	895.55	1.05	pass
E14	6	7187.45	879.96	1.05	pass
Q08	6	7128.78	886.78	1.04	pass
V10	6	7101.5	884.37	1.04	pass
E09	6	7173.89	885.16	1.05	pass
E09	6	7173.89	885.16	1.05	pass
E09	7	7085.33	877.73	1.05	TRUE
L04	7	7255.66	901.81	1.04	pass
M18	7	7224.57	893.15	1.04	pass
Q15	7	7082.18	880.18	1.04	pass
O12	7	7075.61	876.49	1.04	pass
D11	7	7084.11	877.67	1.04	pass
G09	7	7127.69	879.31	1.04	pass
G09	7	7127.69	879.31	1.04	pass
G09	8	7175.13	883.81	1.04	TRUE
H02	8	7173.3	883.57	1.03	pass
H21	8	7134.91	878.76	1.03	pass
S06	8	7156.33	881.31	1.03	pass
D19	8	7140.7	879.48	1.03	pass
D04	8	7155.5	881.34	1.03	pass
M01	8	7172.76	883.86	1.03	pass
Q10	8	7145.45	879.53	1.03	pass
Q17	8	7163.85	881.06	1.03	pass
M20	8	7199.44	886.24	1.03	pass
C08	8	7150.06	880.76	1.03	pass
C08	8	7150.06	880.76	1.03	pass
C08	9	7202.99	884.94	1.03	TRUE
K01	9	7134.58	876.05	1.03	pass
E17	9	7155.55	878.61	1.03	pass
L22	9	7172.51	880.62	1.02	pass
C13	9	7138.59	876.4	1.03	pass
C06	9	7143.81	876.98	1.03	pass
E03	9	7137.24	876.16	1.03	pass
K13	9	7151.53	877.03	1.04	pass
M10	9	7121.33	874.16	1.05	pass
S13	9	7146.16	876.98	1.03	pass
O20	9	7205.05	884.99	1.02	pass
S17	9	7148.61	877.72	1.03	pass
Q02	9	7136.35	876.05	1.03	pass

N04	9	7202.13	884.63	1.02	pass
S08	9	7143.79	876.96	1.03	pass
S08	9	7143.79	876.96	1.03	pass
S08	10	7143.48	875.11	1.04	TRUE
H05	10	7213.84	890.52	1.03	pass
H14	10	7127.13	873.06	1.03	pass
H19	10	7154.45	876.25	1.03	pass
C15	10	7124.63	872.82	1.03	pass
R04	10	7163.08	877.9	1.03	pass
O02	10	7148.69	876.29	1.03	pass
V06	10	7142.33	875.07	1.03	pass
M14	10	7146.14	874.98	1.04	pass
K09	10	7162.83	877.35	1.04	pass
Q12	10	7124.2	872.42	1.04	pass
Q19	10	7150.85	875.86	1.03	pass
U12	10	7135.78	874.13	1.03	pass
N22	10	7139.06	874.77	1.03	pass
U18	10	7136.87	874.36	1.03	pass
S15	10	7140.17	874.76	1.03	pass
B10	10	7135.12	874.12	1.03	pass
B10	11	7116.3	869.73	1.04	TRUE
K07	11	7175.51	877.92	1.04	pass
O06	11	7208.32	880.84	1.04	pass
K15	11	7112.56	869.78	1.04	pass
M12	11	7097.33	868.03	1.06	pass
U05	11	7116.14	870.93	1.04	pass
S10	11	7110.18	869.87	1.04	pass
F11	11	7095.05	868.54	1.04	pass
F06	11	7145.1	877.03	1.03	pass
F19	11	7091.88	867.78	1.03	pass
U14	11	7103.23	869.24	1.04	pass
S19	11	7101.27	869.04	1.04	pass
C17	11	7101.22	869.02	1.04	pass
J22	11	7102.81	869.23	1.04	pass
O18	11	7109.18	870.03	1.04	pass
A12	11	7107.79	869.87	1.04	pass
A12	12	7127.47	868.27	1.05	TRUE
H07	12	7089.42	864.61	1.05	pass
K18	12	7169.28	877.73	1.05	pass
G16	12	7198.61	867.79	1.05	pass
H12	12	7051.19	861.04	1.05	pass
N16	12	7131.65	870.93	1.05	pass
U16	12	7065.88	863.2	1.05	pass

Q21	12	7074.82	864.73	1.05	pass
Q06	12	7131.36	871.03	1.04	pass
M07	12	7156.23	873.45	1.05	pass
U10	12	7072.04	863.91	1.05	pass
W13	12	7072.42	864.04	1.05	pass
W13	13	7160.87	876.21	1.05	TRUE
L05	13	7255.42	883.75	1.04	pass
H09	13	7096.22	865.74	1.04	pass
F14	13	7108.91	871.55	1.04	pass
P14	13	7110.42	870.43	1.04	pass
D10	13	7073.9	867.74	1.04	pass
P08	13	7123.3	868.38	1.04	pass
P08	14	7219.45	878.89	1.04	TRUE
L03	14	7248.78	883.66	1.04	pass
P16	14	7123.17	867.8	1.04	pass
K20	14	7135.29	876.71	1.04	pass
D19	14	7135.88	869.95	1.04	pass
G03	14	7169.81	874.2	1.04	pass
G03	15	7202.09	877.97	1.04	TRUE
D07	15	7246.04	882.93	1.04	pass
D12	15	7221.67	879.64	1.03	pass
J02	15	7284.16	888.11	1.04	pass
E03	15	7239.61	882	1.04	pass
P10	15	7237.56	881.63	1.04	pass
S12	15	7212.31	878.38	1.04	pass
E16	15	7206.68	877.91	1.03	pass
R17	15	7190.53	875.75	1.03	pass
N20	15	7198.06	879.45	1.03	pass
O04	15	7303.79	889.33	1.04	fail0
P04	15	7285.76	888.13	1.04	pass
T07	15	7240.85	881.97	1.04	pass
T07	16	7163.6	874.36	1.04	TRUE
J05	16	7337.84	896.16	1.03	fail0
J04	16	7299.5	892.49	1.03	fail0
L01	16	7242.79	884.78	1.03	pass
F09	16	7219.43	881.84	1.03	pass
H18	16	7146.61	884.2	1.03	pass
H18	17	7188.86	879.49	1.03	TRUE
B07	17	7218.04	880.6	1.03	pass
N01	17	7243.78	883.87	1.03	pass
S05	17	7228.42	882	1.03	pass
M22	17	7200.05	878.29	1.03	pass
T18	17	7204.3	878.83	1.03	pass

V07	17	7216.59	880.33	1.03	pass
P18	17	7161.16	882.39	1.03	pass
R09	17	7219.22	880.17	1.03	pass
T14	17	7196.34	877.87	1.03	pass
T14	18	7143.97	875.24	1.03	TRUE
D05	18	7208.13	880.54	1.02	pass
J05	18	7330.04	895.33	1.02	fail0
C16	18	7178.31	876.67	1.02	pass
A11	18	7192.25	878.36	1.02	pass
G20	18	7169.71	880.05	1.02	pass
K22	18	7180.75	877.68	1.02	pass
G12	18	7171.84	875.93	1.02	pass
G12	19	7166.96	883.2	1.02	TRUE
F05	19	7203.97	880.19	1.02	pass
R03	19	7184.47	877.65	1.02	pass
U05	19	7168.69	879.56	1.02	pass
R07	19	7194.35	878.1	1.02	pass
R14	19	7124.54	878.97	1.02	pass
V11	19	7162.42	878.66	1.02	pass
V16	19	7162.48	879.6	1.02	pass
V16	20	7188.63	878.68	1.02	TRUE
G02	20	7149.65	876.19	1.02	pass
F18	20	7088.57	884.04	1.01	fail0
J20	20	7131.46	890.98	1.01	fail0
E19	20	7104.17	881.07	1.01	fail0
P02	20	7154.93	876.84	1.02	fail0
P02	21	7153.94	878.93	1.02	TRUE
D18	21	7122.48	881.13	1.02	pass
O03	21	7210.59	884.17	1.02	pass
P21	21	7119.97	881.99	1.02	pass
J02	21	7148.78	878.05	1.02	pass
B14	21	7127.57	878.78	1.01	pass
R16	21	7083.05	880.06	1.02	pass
K12	21	7123.2	878.2	1.02	pass
N10	21	7150.4	875.79	1.03	pass
T07	21	7143.47	877.57	1.02	pass
T07	22	7104.41	877.16	1.03	TRUE
T07	23	7146.22	880.71	1.03	TRUE
L02	23	7253.44	890.6	1.03	pass
C07	23	7170.76	879.06	1.03	pass
F03	23	7157.84	878.16	1.03	pass
F18	23	7124.57	884.86	1.03	pass
F18	24	7207.66	885.3	1.02	TRUE

C05	24	7207.13	885.54	1.03	pass
O01	24	7225.76	888.21	1.03	pass
V07	24	7200.96	884.74	1.03	pass
Q05	24	7242.47	890.43	1.03	pass
L21	24	7161.04	892.06	1.03	pass
L21	25	7218.4	888.14	1.02	TRUE
E05	25	7190.24	888.27	1.03	fail0
C10	25	7183.32	885.7	1.02	pass
J21	25	7157.54	898.79	1.02	pass
T16	25	7165.84	888.12	1.02	pass
T16	26	7144.24	897.29	1.02	TRUE
G02	26	7184.63	890.55	1.03	pass
E05	26	7178.65	891.07	1.03	pass
C16	26	7172.62	891.65	1.03	pass
N13	26	7145.8	891.27	1.04	pass
L10	26	7193.87	885.97	1.04	pass
J05	26	7333.28	902.35	1.03	fail0
G20	26	7170.15	893.9	1.03	pass
G20	27	7137.34	891.75	1.05	TRUE
G20	28	7168.59	889.67	1.05	TRUE
J03	28	7276.91	894.46	1.05	pass
C12	28	7150.57	886.17	1.04	pass
A09	28	7169.52	886.55	1.05	pass
O21	28	7136.96	893.35	1.04	pass
P03	28	7230.96	888.44	1.05	pass
E20	28	7155.77	890.26	1.05	pass
E20	29	7258.75	892.97	1.04	TRUE
E20	30	7199.49	891.89	1.04	TRUE
G04	30	7269.48	896.39	1.04	pass
J01	30	7233.1	891.28	1.04	pass
B07	30	7198.05	888.54	1.04	pass
T07	30	7200.13	886.96	1.04	pass
N02	30	7281.64	898.04	1.04	pass
L21	30	7193.62	890	1.04	pass
O09	30	7223.48	889.48	1.05	pass
M16	30	7124.56	898.92	1.04	pass
M16	30	7329.22	905.26	1.05	FALSE
B06	30	7200.86	887.55	1.04	pass
L02	30	7205.61	888.12	1.04	pass
J05	30	7362.71	907.45	1.04	fail0
O11	30	7187.38	885.12	1.05	pass
T05	30	7206.77	887.62	1.04	pass
M21	30	7150.64	899.95	1.04	pass

K16	30	7130.34	901.15	1.04	pass
R18	30	7157.53	891.35	1.04	pass
A13	30	7189.22	888.42	1.04	pass
A13	31	7110.61	903.34	1.04	TRUE
J05	31	7351.32	906.91	1.04	fail0
D07	31	7181.84	896.57	1.04	fail0
C05	31	7185.82	895.47	1.04	fail0
V06	31	7184.82	895.67	1.04	fail0
R05	31	7217.77	890.26	1.04	pass
K05	31	7389.39	912.91	1.04	fail0
L07	31	7292.88	896.75	1.05	pass
L07	32	7252.5	895.63	1.04	TRUE
D17	32	7122.34	899.3	1.04	pass
G13	32	7115.44	896.83	1.04	pass
C10	32	7156.14	894.97	1.04	pass
D06	32	7176.92	891.38	1.04	pass
D06	33	7118.73	895.95	1.04	TRUE
J21	33	7104.07	894.4	1.04	pass
E04	33	7141.91	888.99	1.04	pass
E04	34	7131.82	892.43	1.04	TRUE
L18	34	7223.73	918.03	1.04	pass
K14	34	7062.1	896.19	1.05	pass
K14	35	7253.53	921.55	1.05	TRUE
J05	35	7295.18	901.74	1.05	pass
J05	36	7293.56	901.94	1.05	TRUE
J01	36	7197.18	901.84	1.05	pass
N18	36	7245.54	922.25	1.04	pass
N18	37	7209.63	917.76	1.04	TRUE
G04	37	7279.07	903.18	1.04	pass
O08	37	7243.88	896.28	1.05	fail0
O08	38	7268.99	901.85	1.04	TRUE
L16	38	7179.25	914.61	1.04	pass
C11	38	7156.46	900.54	1.04	pass
D15	38	7126.37	905.88	1.04	pass
T11	38	7159.52	899.68	1.04	pass
T11	39	7144.08	910.42	1.04	TRUE
T11	40	7129.19	900.43	1.04	TRUE
N09	40	7138.05	892.04	1.06	pass
G10	40	7104.13	893.7	1.05	pass
N15	40	7084.51	905.77	1.05	fail0
N15	41	7134.82	887.73	1.06	TRUE
N14	41	7031.3	897.43	1.06	fail0
J15	41	7083.31	904.79	1.06	pass

J15	42	7052.99	902.85	1.05	TRUE
N15	42	7077.26	904.56	1.06	pass
N02	42	7175.98	890.82	1.05	pass
K08	42	7142.9	889.1	1.06	pass
K08	43	7177.45	889.52	1.06	TRUE
K08	44	7125.91	896.81	1.06	TRUE
J10	44	7120.54	888.2	1.06	pass
D08	44	7121.04	887.98	1.05	pass
G14	44	7087.74	898.2	1.06	pass
G14	45	7178.73	895.97	1.06	TRUE
G14	46	7062.24	890.7	1.06	TRUE
O08	46	7102.38	879.01	1.06	pass
J06	46	7195.17	892.02	1.06	pass
J17	46	7166.55	913.93	1.05	pass
J17	47	7143.96	892.72	1.06	TRUE
J17	48	7102.83	899.08	1.05	TRUE
J12	48	7050.23	894.83	1.06	pass
R13	48	7031.17	893.67	1.05	pass
R13	49	7008.89	890.55	1.06	TRUE
J20	49	7207.53	918.98	1.05	pass
J20	50	7201.19	918.04	1.05	TRUE
N05	50	7242.5	894.01	1.05	pass
G06	50	7138.14	898.89	1.05	pass
G06	50	7339.3	908.39	1.05	FALSE
N03	50	7207.91	894.33	1.05	pass
F07	50	7090.66	894.44	1.05	fail0
T09	50	7058.54	900.78	1.05	pass
T09	51	7203.82	890.73	1.05	TRUE
M15	51	7173.37	910.76	1.05	pass
E11	51	7072.26	899.68	1.04	pass
F17	51	7227.83	919.63	1.04	fail0
F17	52	7123.88	904.11	1.05	TRUE
Q09	52	7038.65	888.98	1.05	pass
P13	52	7060.25	897.19	1.05	pass
P13	53	6990.69	886.57	1.06	TRUE
J08	53	7101.82	879.3	1.05	pass
J08	54	7093.74	881.17	1.05	TRUE
G08	54	7116.68	892.09	1.05	pass
G15	54	7144.02	900.13	1.05	pass
G15	55	7082.72	892.68	1.04	TRUE
W09	55	7023.32	888.82	1.04	pass
T13	55	7006.37	886.69	1.04	pass
T13	56	6994.72	884.74	1.04	TRUE

M05	56	7235.84	893.5	1.04	pass
E13	56	7222.4	907.46	1.04	pass
E13	57	7155.1	892.17	1.03	TRUE
P11	57	7055.54	878.57	1.04	pass
P11	58	7053.14	874.86	1.05	TRUE
T08	58	7047.1	874.22	1.04	pass
H06	58	7191.68	897.68	1.04	pass
M17	58	7152.4	897.76	1.04	pass
M17	59	7072.48	878.32	1.04	TRUE
M17	60	7054.94	880.72	1.04	TRUE
P19	60	7152.55	891.36	1.03	pass
O05	60	7248	895.31	1.04	pass
H10	60	7050.12	885.8	1.04	pass
T16	60	7048.96	877.56	1.03	fail0
T16	61	7142.35	880.95	1.03	TRUE
T16	62	7069.12	876.7	1.03	TRUE
F17	62	7135.95	891.79	1.04	fail0
F08	62	7186	892.17	1.03	pass
F08	62	7186	892.17	1.03	pass
F08	63	7074.37	881.4	1.03	TRUE
F17	63	7122.45	887	1.04	fail0
G19	63	7109.82	890.63	1.03	pass
W11	63	7015.08	874.7	1.03	pass
Q14	63	7013.62	867.94	1.04	pass
R08	63	7047.64	869.53	1.04	pass
L11	63	7012.8	874.63	1.06	pass
T16	63	7026.4	877.15	1.03	pass
R19	63	7038.78	873.59	1.03	pass
K03	63	7292.72	903.23	1.03	fail0
Q04	63	7118.48	881.49	1.03	fail0
Q04	64	7036.18	877.94	1.04	TRUE
F16	64	7122.36	886.75	1.04	pass
K05	64	7269.55	903.63	1.04	fail0
K05	65	7097.46	882.34	1.04	TRUE
Q11	65	6938.01	863.91	1.05	pass
P07	65	7084.44	873.31	1.04	pass
K03	65	7238.77	894.94	1.04	pass
G21	65	7016.13	880.99	1.04	pass
G21	66	7259.31	896.4	1.05	TRUE
G21	67	7042.68	872.43	1.04	TRUE
L20	67	7225.4	909.74	1.03	fail0
F10	67	7104.08	886.33	1.04	pass
G06	67	7170.75	912.44	1.04	pass

M08	67	7129.63	879.52	1.05	pass
B09	67	7027.72	876.94	1.04	pass
J13	67	7060.02	869.95	1.05	pass
J13	67	7184.86	912.91	1.04	FALSE
J16	67	7135.05	889.33	1.04	pass
J07	67	7169.26	891.52	1.04	pass
E06	67	7093.69	888.71	1.04	fail0
J11	67	7021.04	868.27	1.05	pass
J11	67	7050.41	877.22	1.04	FALSE
J18	67	7258.74	918.75	1.03	fail0
H04	67	7225.88	914.41	1.04	fail0
K05	67	7344.09	912.14	1.04	fail0
F04	67	7126.96	891.99	1.04	fail0
B11	67	7025.52	883.79	1.04	pass
E05	67	7033.11	868.81	1.04	fail0
L06	67	7281.98	901.09	1.04	pass
Q16	67	7016.94	873.37	1.04	pass
M13	67	6980.2	869.13	1.06	pass
V09	67	7029.28	868.96	1.04	pass
T12	67	6999.19	865.26	1.04	pass
V15	67	7018.73	867.64	1.04	pass
B15	67	7029.5	870.26	1.04	pass
B15	68	7001.74	871.63	1.04	TRUE
B15	69	7046.33	876.24	1.03	TRUE
L20	69	7111.91	894.55	1.03	pass
N05	69	7312.57	911.62	1.04	fail0
E06	69	7098.88	888.68	1.03	fail0
N11	69	7026.7	870.61	1.06	pass
N11	70	7047.84	884.99	1.06	TRUE
F17	70	7149.5	895.36	1.05	fail0
H04	70	7215.62	911.12	1.05	fail0
E06	70	7079.68	883.81	1.05	fail0
F04	70	7114.13	887.79	1.05	fail0
E08	70	7241.66	891.52	1.05	fail0
E05	70	7018.47	874.33	1.05	pass
H03	70	7034.17	873.35	1.05	pass
D14	70	7189.67	888.33	1.05	fail0
E12	70	7186.38	907.8	1.05	fail0
N05	70	7309.64	909.26	1.06	fail0
N06	70	7225.25	894.31	1.06	pass
S14	70	6936.48	871.79	1.06	pass
S09	70	7016.07	867.95	1.06	pass
Q20	70	7017.79	882.81	1.05	pass

O15	70	7024.74	881.14	1.06	pass
G17	70	7211.5	898.98	1.05	pass
G17	70	6966.87	870.11	1.06	FALSE
J18	70	7293.25	923.27	1.05	fail0
E15	70	7306.87	894.25	1.05	fail0
D09	70	7122.56	896.71	1.05	fail0
F08	70	7020.74	874.35	1.05	pass
B13	70	7005	881.47	1.05	fail0
G03	70	7001.64	876.02	1.05	fail0
F13	70	7156.9	886.17	1.05	pass
A13	70	7019.67	874.7	1.05	pass
M03	70	7337.61	912.5	1.05	fail0
Q04	70	7121.8	881.76	1.06	pass
V12	70	7001.96	872.5	1.05	pass
S16	70	6965.49	875.83	1.05	pass
S07	70	7044.5	871.7	1.06	pass
M04	70	7452.14	924.85	1.06	fail0
O17	70	7186.34	892.77	1.06	pass
O17	71	6960.98	863.58	1.05	TRUE
O17	72	6932.01	864.83	1.04	TRUE
J18	72	7199.57	911.33	1.03	pass
K04	72	7285.67	909.1	1.03	fail0
K04	73	7170.95	906.87	1.03	TRUE
K05	73	7269.75	903.7	1.04	pass
L01	73	7016.4	887.86	1.04	fail0
L01	74	7260.87	901.81	1.04	TRUE
J07	74	7203.7	908.74	1.04	pass
J14	74	7071.66	891.77	1.04	pass
N19	74	7335.75	917.24	1.03	fail0
R12	74	7003.58	878.72	1.04	pass
R12	75	7073.13	888.9	1.05	TRUE
B09	75	7038.18	890.18	1.04	pass
E19	75	7036.92	885.38	1.04	pass
E19	76	7005.46	880.05	1.04	TRUE
E06	76	7105.13	899.35	1.04	fail0
M08	76	7117.84	892.51	1.05	pass
O19	76	7182.82	897.72	1.04	pass
H04	76	7227.58	925.86	1.04	fail0
H04	77	7058.12	880.33	1.04	TRUE
F10	77	7077.55	887.35	1.04	pass
D13	77	7138.9	888.99	1.04	pass
K10	77	7042.43	886.17	1.06	pass
K10	78	7260.58	906.38	1.06	TRUE

K10	79	6965.57	872.84	1.05	TRUE
Q20	79	7031.36	877.02	1.05	pass
E06	79	7106.09	891.37	1.05	fail0
H04	79	7179.17	916.88	1.06	pass
F07	79	7238.92	897.2	1.06	pass
F07	80	7177.37	918.58	1.05	TRUE
M16	80	7103.46	888.82	1.05	pass
M16	81	7115.19	886.73	1.05	TRUE
F17	81	7125.7	886.64	1.04	fail0
N05	81	7291.59	920.01	1.05	pass
H17	81	7095.81	908.01	1.04	pass
H17	82	7086.76	898.83	1.04	TRUE
O13	82	6986.85	888.33	1.06	pass
O13	83	6984.32	885.95	1.06	TRUE
D09	83	7105.96	898.35	1.04	pass
F04	83	7100.35	914.67	1.05	fail0
F17	83	7190.86	921.7	1.05	fail0
F17	84	7053.96	894.15	1.04	TRUE
E15	84	7285.09	896.74	1.04	pass
M03	84	7308.44	915.77	1.05	fail0
S04	84	6989.39	890.62	1.05	pass
S04	85	7181.89	883.11	1.04	TRUE
P17	85	7184.09	904.42	1.05	pass
G06	85	7202.33	922.63	1.04	pass
T07	85	7097.39	879.48	1.04	pass
T07	86	7049.89	898.82	1.04	TRUE
M03	86	7280.86	928.26	1.04	pass
M03	87	7256.6	923.69	1.04	TRUE
J16	87	7143.96	897.87	1.04	pass
J11	87	7256.6	923.69	1.04	fail0
J11	88	7159.58	895.2	1.05	TRUE
O07	88	7183.93	908.56	1.05	pass
O07	89	7168.87	904.91	1.05	TRUE
F17	89	7302.46	917.36	1.03	fail0
G17	89	7347.58	928.38	1.04	fail0
B17	89	7048.58	889.87	1.04	pass
J19	89	7255.87	944.61	1.04	fail0
K21	89	7022.96	890.55	1.04	fail0
L19	89	7354.5	921.91	1.04	fail0
L22	89	7016.33	892.44	1.04	fail0
L17	89	7269	909.87	1.04	pass
E06	89	7106.94	914.63	1.04	pass
E06	90	7149.15	896.95	1.04	TRUE

E06	91	7051.56	898.07	1.04	TRUE
B13	91	7048.88	897.26	1.03	pass
R15	91	7114.18	886.59	1.04	pass
S09	91	6992.77	889.08	1.04	pass
W12	91	7039.53	896.02	1.04	pass
P12	91	7052.67	886.57	1.06	pass
P12	92	7003.18	878.76	1.07	TRUE
P12	93	6941.16	885.69	1.05	TRUE
G11	93	7171.15	897.02	1.04	pass
F17	93	7250.33	905.37	1.03	fail0
F17	94	7137.72	893.44	1.04	TRUE
J19	94	7203.71	933.31	1.03	pass
Q07	94	7004.91	886.49	1.05	pass
Q07	95	7037.41	911.51	1.04	TRUE
E08	95	7481.71	917.86	1.03	fail0
H08	95	7308.55	917.21	1.04	fail0
L08	95	7057.31	895.37	1.04	pass
L08	96	7022.61	893.98	1.05	TRUE
D14	96	7249.95	911.28	1.03	fail0
F17	96	7209.22	938.28	1.03	fail0
O22	96	7015.03	907.28	1.04	pass
M19	96	7299.96	935.7	1.04	fail0
G17	96	7278.78	947.67	1.03	pass
R18	96	7025.01	902.04	1.04	pass
N17	96	7361.57	923.29	1.04	fail0
J04	96	7226.5	940.6	1.04	pass
J04	97	7078.22	925.42	1.03	TRUE
J04	98	7014.98	916	1.04	TRUE
E12	98	7322.2	916.78	1.03	fail0
J13	98	7071.92	919.62	1.04	pass
O15	98	7114.1	918.49	1.04	pass
N19	98	7291.63	939.13	1.03	pass
O09	98	7033	911.09	1.06	pass
D14	98	7221.27	922.55	1.03	fail0
E10	98	7372.91	917.37	1.04	fail0
B08	98	7083.45	914.07	1.03	pass
F15	98	7397.37	936.5	1.03	fail0
H08	98	7351.3	936.41	1.05	fail0
C14	98	7006.99	914.34	1.03	pass
O04	98	7264.65	930.29	1.04	pass
E18	98	7024.88	918.95	1.03	pass
T17	98	6986.7	912.38	1.04	pass
K21	98	7015.07	917.75	1.03	pass

W10	98	7006.71	911.45	1.04	pass
S11	98	6941.37	901.31	1.04	pass
F04	98	7176.05	938.39	1.03	fail0
V14	98	6987.31	910.85	1.04	pass
G07	98	7467.37	954.31	1.04	fail0
U07	98	7001.52	908.62	1.04	pass
E05	98	7036.52	913.15	1.03	pass
J08	98	7253.59	932.9	1.05	pass
J08	98	7077.9	897.49	1.05	FALSE
E08	98	7464.16	929.72	1.04	fail0
L19	98	7429.73	958.61	1.03	fail0
L14	98	7087.94	922.47	1.04	pass
V17	98	7004.01	912.64	1.04	fail0
P02	98	7054.02	917.33	1.04	pass
N17	98	7353.43	934.7	1.03	fail0
U13	98	6959.87	908	1.04	pass
S20	98	6997.62	914.18	1.04	pass
C10	98	7022.06	912.12	1.03	pass
C15	98	7009.55	913.81	1.03	pass
R10	98	6963.51	903.08	1.05	pass
O20	98	7007.63	915.73	1.04	pass
N06	98	7339.97	931.1	1.04	fail0
P15	98	7090.07	915.6	1.04	pass
T06	98	7006.46	909.56	1.04	pass
K22	98	7012.7	913.82	1.04	fail0
L22	98	7016.59	912.64	1.04	fail0
J21	98	7006.78	914.88	1.04	fail0
U17	98	7018.18	912.99	1.04	fail0
V09	98	7015.77	913.18	1.04	fail0
W09	98	7015.9	913.14	1.04	fail0
M04	98	7592.34	953.71	1.03	fail0
E06	98	7018.8	912.56	1.04	fail0
K02	98	7039.56	915.2	1.04	pass
F05	98	7032.95	912.79	1.04	pass
F05	98	7032.95	912.79	1.04	pass
F05	98	7044.33	890.84	1.05	FALSE
H15	98	7299.05	939.99	1.03	fail0
D16	98	7014.66	916.1	1.03	pass
N14	98	7073.84	916.95	1.06	pass
C09	98	7031.11	911.59	1.03	pass
U11	98	6971.82	906.55	1.04	pass
L21	98	7012.35	913.39	1.04	fail0
M19	98	7306.81	947.06	1.03	fail0

M20	98	7026.69	919.31	1.03	pass
P04	98	7028.51	913.34	1.04	pass
M02	98	7036.99	914.44	1.04	pass
B13	98	7014.02	912.98	1.04	fail0
L11	98	7012.2	914.04	1.04	fail0
U15	98	7013.7	912.87	1.04	fail0
S14	98	6986.24	906.48	1.04	pass
V16	98	7019.17	913.1	1.04	fail0
V07	98	7016.59	913.56	1.04	fail0
T18	98	7019.64	912.89	1.04	fail0
U06	98	7015.59	913.38	1.04	fail0
F19	98	7009.63	916.3	1.04	pass
T07	98	7015.42	913.2	1.04	fail0
E04	98	7006.04	913.67	1.04	fail0
T05	98	7014.98	913.35	1.04	fail0
R20	98	7015.76	912.9	1.04	fail0
U18	98	7019.22	912.95	1.04	fail0
D05	98	7013.55	913.04	1.04	fail0
W14	98	7006.28	912.21	1.04	fail0
F19	98	7006.28	912.21	1.04	fail0
F19	99	7001.8	899.19	1.05	TRUE
E12	99	7308.27	914.48	1.02	fail0
B12	99	6951.59	909.55	1.03	fail0
E08	99	7421.69	919.91	1.02	fail0
A11	99	6946.76	909.63	1.03	fail0
E10	99	7360.4	907.23	1.02	fail0
A09	99	6948.36	909.81	1.03	fail0
F15	99	7363.74	933.19	1.02	fail0
A13	99	6946.02	909.44	1.03	fail0
H15	99	7253.04	936.62	1.03	pass
E09	99	7033.43	907.11	1.03	pass
C12	99	6947.18	909.62	1.03	fail0
M04	99	7527.56	949.44	1.03	fail0
N06	99	7233.04	919.95	1.04	fail0
S04	99	6945.89	909.45	1.03	fail0
O01	99	6953.07	910.43	1.03	fail0
R03	99	6950.79	910.11	1.03	fail0
R04	99	6940.34	908.66	1.03	fail0
R05	99	6948.41	909.77	1.03	fail0
S03	99	6950.68	910.09	1.03	fail0
M06	99	6979.45	905.49	1.03	pass
T04	99	6950.97	910.13	1.03	fail0
M22	99	6945.19	908.81	1.03	fail0

L12	99	6958.8	909.27	1.05	pass
N17	99	7335.31	930.71	1.05	fail0
B17	99	6947.9	909.72	1.03	fail0
G21	99	6946.49	907.26	1.03	fail0
H21	99	6951.31	910.66	1.03	fail0
V17	99	6943.87	909.18	1.03	fail0
C18	99	6943.84	909.13	1.03	fail0
Q20	99	6948.08	909.02	1.03	fail0
Q21	99	6945.95	909.2	1.03	fail0
T19	99	6946.65	909.48	1.03	fail0
V16	99	6948.44	909.75	1.03	fail0
L17	99	6990.82	910.18	1.03	fail0
U09	99	6903.95	901.57	1.03	fail0
G03	99	6948.8	908.7	1.03	fail0
F03	99	6951.24	910.19	1.03	fail0
H02	99	6944.64	909.09	1.03	fail0
A10	99	6947.18	909.63	1.03	fail0
B06	99	6949.83	910.01	1.03	fail0
C06	99	6947.39	909.65	1.03	fail0
E03	99	6950.8	910.13	1.03	fail0
A12	99	6946.53	909.55	1.03	fail0
C05	99	6950.4	910.08	1.03	fail0
A14	99	6945.62	909.41	1.03	fail0
T09	99	6952.1	910.4	1.03	fail0
G02	99	6952.91	910.43	1.03	fail0
E13	99	6943.72	908.73	1.03	fail0
L18	99	6964.24	911.24	1.03	fail0
W12	99	6945.94	909.44	1.03	fail0
L12	99	6945.94	909.44	1.03	fail0
L12	100	7198.94	926.28	1.03	TRUE

A4.1 Refueling Log